REPUBLIC OF TURKEY

ALTINBAŞ UNIVERSITY

Institute of Graduate Studies

Information Technologies

PERFORMANCE ENHANCEMENT OF MICROSTRIP PATCH ANTENNA FOR INDOOR APPLICATIONS

Mohammed SHAFEAY

Master's Thesis

Supervisor

Asst. Prof. Dr. Sefer KURNAZ

Istanbul, 2021

PERFORMANCE ENHANCEMENT OF MICROSTRIP PATCH ANTENNA FOR INDOOR APPLICATIONS

Mohammed SHAFEAY

Information Technologies

Master's Thesis

ALTINBAŞ UNIVERSITY

2021

The thesis titled "PERFORMANCE ENHANCEMENT OF MICROSTRIP PATCH ANTENNA FOR INDOOR APPLICATIONS" prepared by "MOHAMMED SHAFEAY" and submitted on (29/12/2021) has been **accepted unanimously** for the degree of Master of Science in Electrical and Computer Engineering.

Asst. Prof. Dr. Sefer KURNAZ

Supervisor

Thesis Defense Jury Members:

Asst. Prof. Dr. Sefer KURNAZ	Faculty of Engineering and Architecture, Altinbas University	
Asst. Prof. Dr. Muhammad ILYAS	Faculty of Engineering and Architecture, Altinbas University	
Prof. Dr. A. Mesut RAZBONYALI	Faculty of Engineering and Natural Sciences, Maltepe University	

I hereby declare that this thesis meets all format and submission requirements of a Master's thesis.

Accepted by Altınbaş University Institute of Graduate Studies on the following date:

29/12/2021

I hereby declare that all information in this document has been obtained and presented in accordance with academic rules and ethical conduct. I also declare that, as required by these rules and conduct, I have fully cited and referenced all material and results that are not original to this work.

Mohammed SHAFEAY

ACKNOWLEDGEMENTS

First of all, I thank Allah Almighty for his mercy, grace and generosity in completing my higher education. I extend my heartfelt thanks to my dear supervisor, Dr. Sefer KURNAZ, for his support and paternalistic dealings during the period of his supervision of my thesis. I would like to thank my family, my father and my mother for their prayers and their unlimited support for me, and I would like to thank my dear wife for the love, encouragement and support. Finally, I would like to thank all the friends and the teaching and administrative staff at our university for their help and support.

ABSTRACT

PERFORMANCE ENHANCEMENT OF MICROSTRIP PATCH ANTENNA FOR INDOOR APPLICATIONS

Shafeay, Mohammed

M.Sc., Electrical and Computer Engineering, Altınbaş University,

Supervisor: Asst. Prof. Dr. Sefer KURNAZ

Co-Supervisor:

Date: September / 2021

Pages: 53

There are many structures of the antennas utilised in wireless communication applications, one of the most widely known and utilised is the Microstrip Patch Antenna (MPA). This antenna is most recognised due to its benefits in terms of geometry configuration that makes it fitting for various of the communication via distance application. The small weight of this antenna structure and the appropriateness for mixture with many of the microwave applications is very useful as well as required. This antenna has flawed by the narrow bandwidth and the low or the poor gain issues. Consequently, to utilise this antenna properly the mentioned issues should be optimised to boost the antenna performance. In this study, we will introduce a design of an MPA with a rectangular patch shape at an operating frequency of 60GHz employing the finite integration technique that is offered by the Computer Simulation Technology (CST) antenna simulation package. This frequency band is chosen due to the free license operation and the ability to get a higher data rate for the indoor application. In order to get the best connection and avoid mismatching issues, the inset-fed scheme is used to feed the simulated antenna; this is the method easy to manufacture and provides naivety modeling and impedance matching. In order to optimise the simulated antenna realisation, the mushroom-like Electromagnetic Bandgap (EBG) square cells are introduced. These

cells are implanted over the antenna substrate and connected with the antenna ground plane through the vias. Finally, a performance comparison between utilising the mushroom-like EBG structure and the Frequency Selective Surface (F) will be studied.

Keywords: 60 GHz, FSS, Indoor Applications, EBG, Microstrip Patch Antenna.

TABLE OF CONTENTS

Pages

LIST OF TABLES

Page

LIST OF FIGURES

Page

ABBREVIATIONS

BW	: Bandwidth
CST	: Computer Simulation Technology
EBG	: Electromagnetic Bandgap
FSS	: Frequency Selective Surface
HD	: High Definition
HDMI	: High-Definition Multimedia Interface
ISI	: Inter-Symbol Interference
LoS	: Line of Sight

MAC : Media Access Control

MPA : Microstrip Patch Antenna mm-waves

: Millimetre Waves

NLoS : None Line of Sight

VSWR : Voltage Standing Wave Ratio

WiGig : Wireless Gigabit Alliance

: Wireless Local Area Network

WLAN

1. GENERAL INTRODUCTION

1.1 OVERVIEW

The wireless communications applications have grown at an unmatched rate in recent years, owing to the expansion of venerable and "bandwidth-hungry" technologies. From pager systems and cell phones to cutting-edge personal digital assistants, set-top-boxes, personal computers, and other tools that are able for producing the huge-speed multimedia purport while associated with a fast and secure broadband wireless local area network or the wireless personal area network. With the developments in the technology the wireless networks were expanded their capability many times each five years in to keep up with the massive number of data traffic needed by the most modern and high bitrate multimedia requirements [1]. The network operators are predicted to reach about1 Gbit/sec speed once utilising the millimetre waves (mm-waves) in the not-too-distant future, the evolutions happened in the wireless communications can be summarised in Figure 1.1.

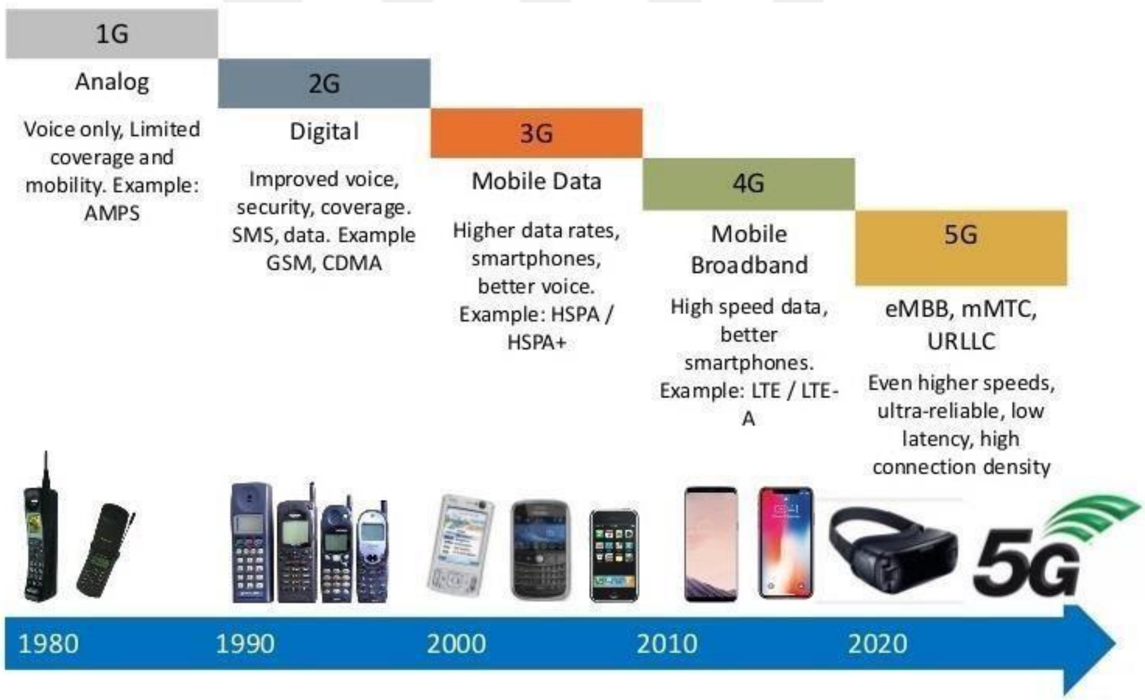

Figure 1.1: Wireless communications evolution.

Many services and applications need extremely large bit rates, which will most probable rise in the next few years. The apps comprise un-compressed instant of high-definition television, audio or video transmission, gaming, and the rapid file transfers. These enforcements are currently reliant on the utilisation of the guided media technologies (i.e. wire transmission), like as the universal serial bus 2.0, HDMI, and FireWire. Contemporaneous the wireless criteria, on the other hand, are only able to back the usual data traffic in the Bluetooth and the wireless local area network moreover are obviously unqualified to back such high data rates. In this meaning, the mm-waves band is considered to be the extreme hopeful wireless communications applicant for the next generations to achieve many of the gigabit rates via the air media as illustrated in Figure 1.2.

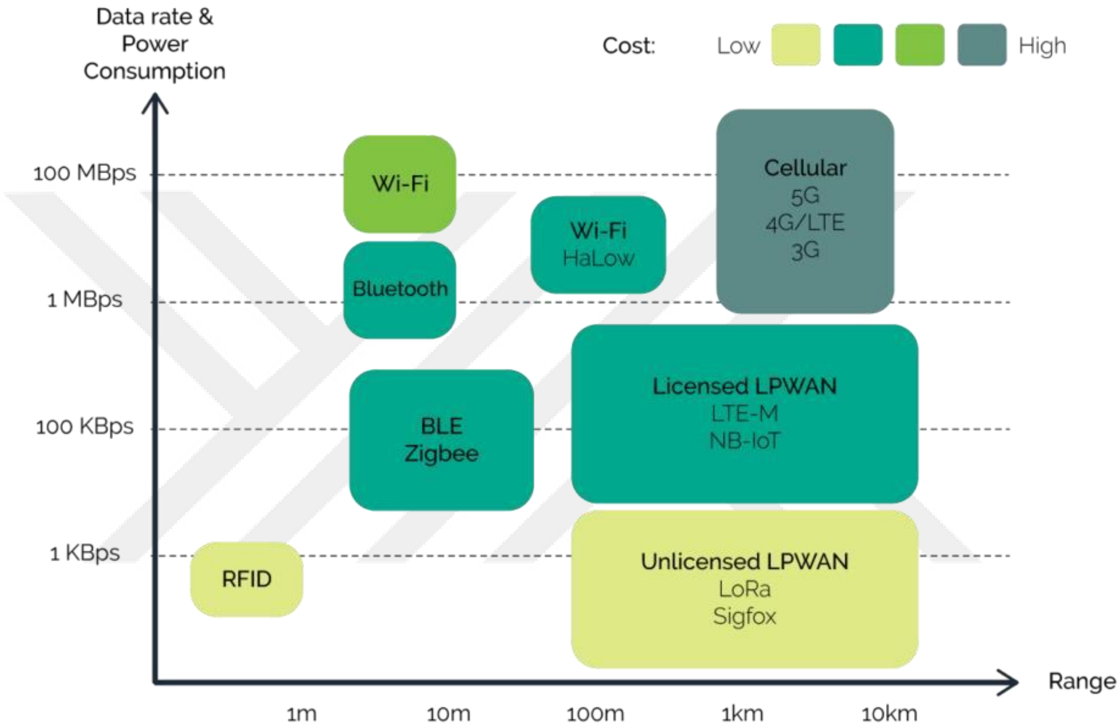

Figure 1.2: Data rates versus the covering range.

The availability of the license-free spectrum near the 7GHz, low interference ratio, a compactsized antenna, and different technology enablers turn out the 60GHz band the most hopeful competitor to supporting many Gb/sec data rates. For the Microstrip Patch Antenna (MPA) because of the small distance among the radiation elements, metal layers and substrates, the design and construction of 60GHz antennas with a size of just a few microns was difficult. Since the losses of the radiation and of the conduction are enormously high due to the absorption of the substrate and to conducting current. This makes the antenna suffering from the poor gain and efficiency. The MPA has numerous benefits which will be presented in the next chapter that pulled the researchers' attention [2].

1.2 WIRELESS COMMUNICATIONS AT 60GHZ

Since the 1990s, there has been a rising in the need for the high data rates and modern technologies were invented for high-speed communications. This improved the growth of new lightweight, roving and affordable appliances. The bandwidth inclination of users towards such technologies has been considerably raised with all the benefits of these technologies. This manner allowed offices and homes to be free of cable clutter. The several of the obtainable bands such as the 2.4 and 5GHz quickly ran out of spectrum Because of the high employment of bandwidth. This high need has sparked benefits in looking into the possibility of using high frequencies with large bandwidths to facing the mentioned problem. The 60 GHz band is an example, with plenty of license-free spectrum obtainable up to 7GHz. Data rates of many Gb/sec are possible with communication systems operating in this band [3]. As a result, 60GHz is a useful competitor for providing high-data-rate within a short-range communication (e.g. indoor applications). The relation between the bandwidth and the capacity can be expressed by utilising the Shannon's equation, as follows [4]:

$$C = B.W \times \log_2(1 + SNR) \tag{1.1}$$

Where:

C: Is referring to the capacity of the channel;

B.W: Is referring to the bandwidth;

SNR: Is referring to the signal to noise ratio.

The 60 GHz band is being touted as a possible competitor for many gigabit data rates. The summarised following technology enablers are primarily responsible for this:

a) The most charming feature of this frequency band can be summarised by the presence of a large electromagnetic spectrum which up to 7GHz and nearly the 60 GHz, such bands are completely free from licenses in the worldwide. As shown in Figure 1.3, where the careful spectral stretching changes according to the country rules and regulations [5].
b) The High-frequency systems require extremely directive or extremely concentrated antennas for overcoming the influences of air absorption, a more explanation for this parameter will be clearly presented in the next chapter. For 60 GHz, consequently, it is possible to manufacture a highly directed, narrow beam, and small MPA. The narrow beam

has different important advantages, making connections extremely impregnable to interfere from the other broadcasting stations. The result is a higher degree of synthesis, meaning a low-cost device [6].

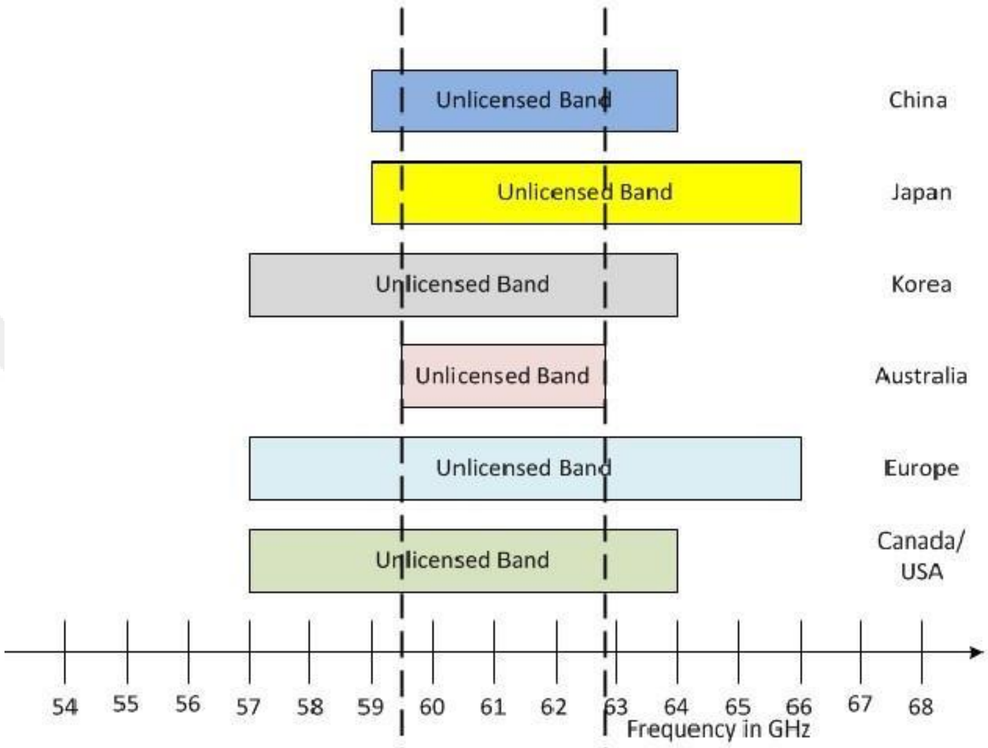

Figure 1.3: License-free frequency.

c) The oxygen absorption characteristic leads to making the 60GHz in many applications extra attractive. The wave of the 60GHz is considerably subjected to be attenuated for the applications that require a long-distance because of the large oxygen absorption. The wave can't consequently progress far away from the transmitter. The reduction of 60GHz due to the absorption is illustrated in Figure 1.4. As presented in Figure 1.5, due to the oxygen absorption characteristic permits a higher frequency re-use at 60GHz [7].

d) The 60 GHz signal could be thought of as being restricted to a single room, in other words, employed for indoor applications. The 60 GHz communications are supposed to have a small number of interference levels due to the sharp propagation and permeation losses, as well as the high directionality of sections operating at these frequencies.

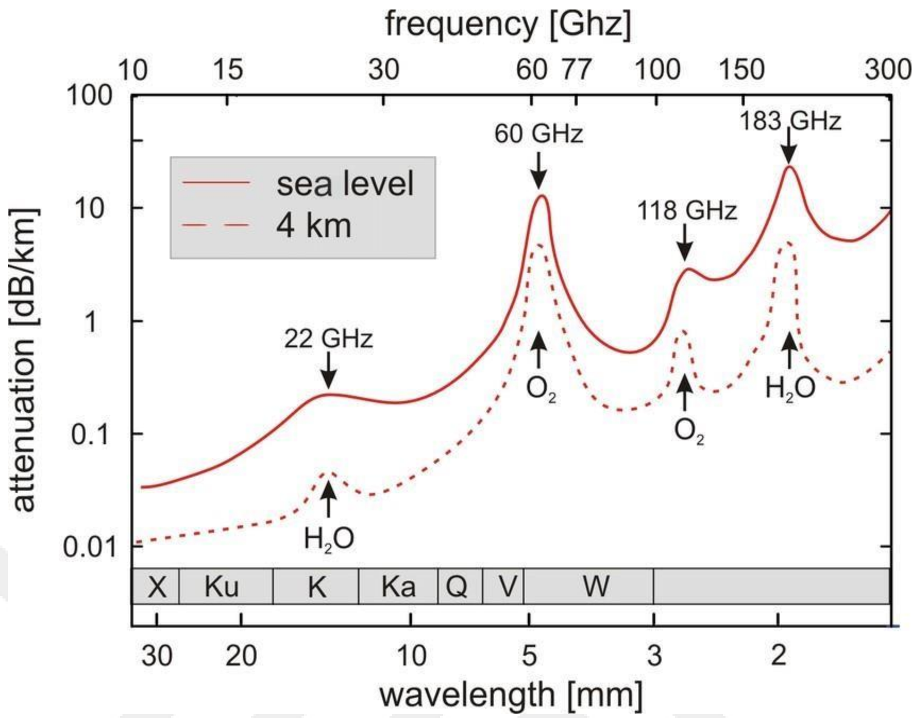

Figure 1.4: Oxygen absorption for mm-waves.

e) Low-cost front end technology: in various previous studies with 60 GHz technology, lowcost, very incorporated, and low extent front-end technology for 60 GHz radios has immediately been described.

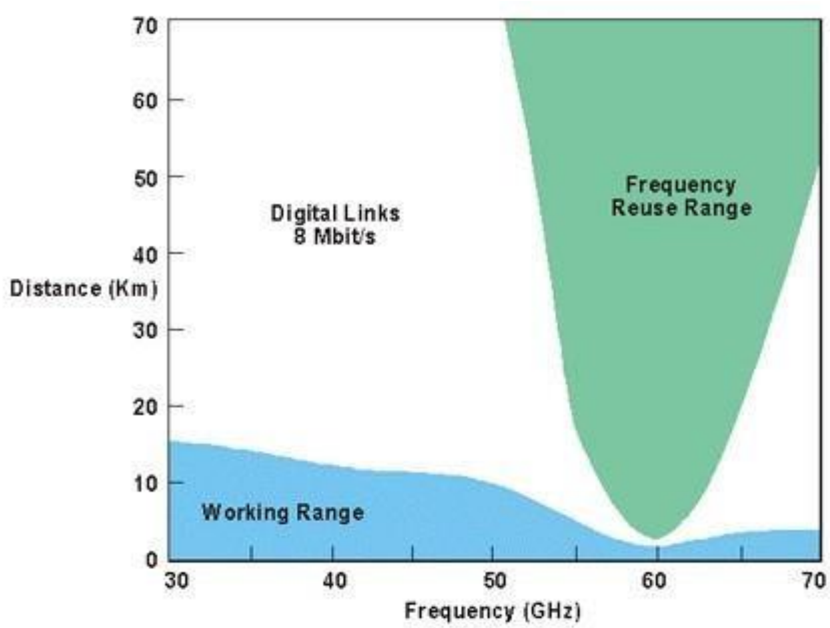

Figure 1.5: The frequency reuse for 60GHz.

With the previously mentioned 60GHz advantages, this band faces a number of issues that must be overcome in order to reach its complete possibility. The following are a few of them [8], [9]:

a) Poor link budget: Propagation causes significant attenuation in the 60 GHz band. The freespace path loss at 60GHz is in the range about 20-30 dB which considered higher than that in the wireless local area network that working on the 2.5GHz, even if oxygen absorption is ignored for short-range radio connections. Moreover, the whole noise power is incomparably larger than that in the systems that are working at slash frequencies due to the very great transmission BW, up to 2.16GHz. As a result of these factors, the link budget is poor.
b) Line-of-Sight (LOS) requirement: Another significant issue with 60GHz radios is requirement of the LoS transmission, where the signal blockage could happen because of the existence of the chattels, objects, or people in the propagation area. The existence of a human on the LoS route regularly results in a shadowing loss of more than 20 decibels. Nevertheless, in the None LoS ($NLoS$) situations, 60GHz radios must comprise a procedure for setting secure communication connections.
c) Indoor radio propagation at 60GHz is characterised by an altitude level of scattering with reflections, appearing in multipath frequency-selective radio channels. Because of this characteristic, 60GHz communications are more suitable to experience Inter-Symbol Interference (ISI), which can critically deteriorate system enforcement if usual countermeasures are not implemented.

1.3 APPLICATIONS OF 60GHZ BAND

The utilisation of the 57-64GHz frequency band for Gigabit short-range wireless communication systems is a hopeful solution to overcome the problems of the need for the high speed data rate. Throughout the world, the licensed free BW as previously mentioned is up to 7GHz has been designated for several communication applications, and standardisation is progressing beneath the IEEE pattern 802.15.3c. Many of the applications can be working in such frequency band, some of which are summarised as follows [9], [10]:

a) **In the airplanes:** The 57-64GHz frequency band that can be utilised for the onboard systems at aeroplanes which have practically employed the wire transmission among the drawbacks in the terms of lower versatility and large establishment costs/efforts. Such drawbacks could be reduced by the construction of a wireless system. Nevertheless, the high need for the high data distribution for audio and video on demand within a big aeroplane with numerous passengers, besides the fact that the system necessity is operable global, has made it complicated to find a commercially available wireless pointtomultipoint solution. Consequently, the central purpose of the wireless transmission system in the aeroplane environment is to demonstrate the abilities of the 60GHz WLAN to afford a really high transmission rate in a two-way communication link, Figure 1.6 illustrates the wirelessly media access control (MAC).

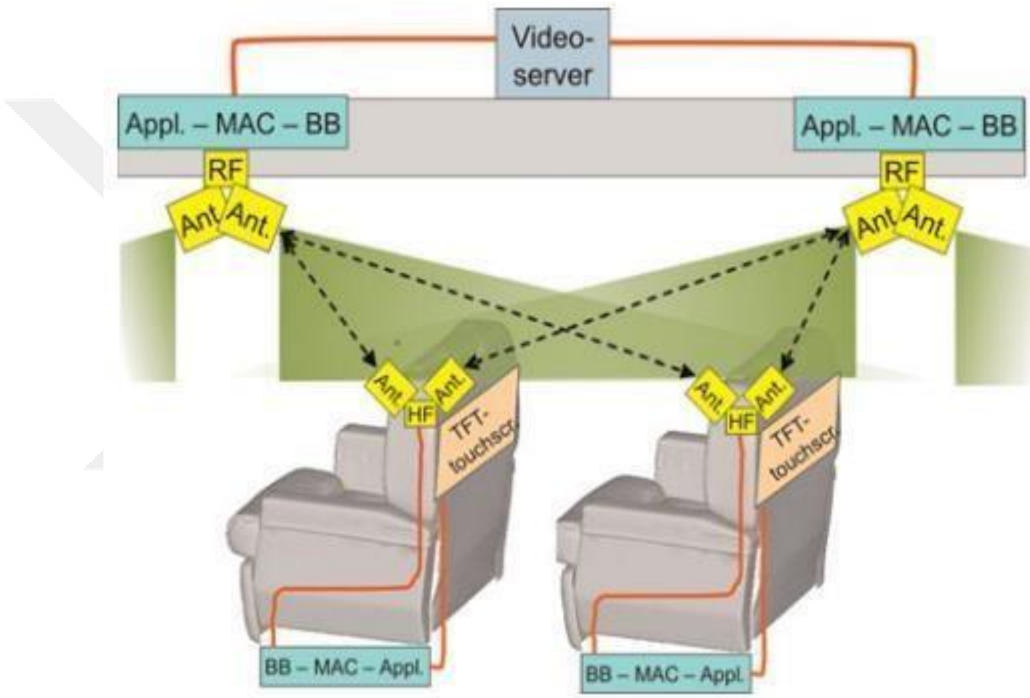

Figure 1.6: Wireless multimedia transmission in the aeroplane.

b) Wireless Gigabit Alliance (WiGig): The WiGig technology or the 60 GHz Wi-Fi, is a technology that commits to an assemblage of 60 GHz wireless network standards. It involves the contemporary IEEE 802.11ad standard and furthers the expected IEEE 802.11ay standard. The WiGig technology extends the practice for virtual reality, multimedia streaming, online gaming, high-definition video transmission, and enterprise applications demanding a high speed, data-intensive transmission. The WiGig enables the Wi-Fi tools to reach the uncongested 60GHz frequency band with broad channels to transfer data significantly at multi-Gb/Sec speeds. The user's interest in the extended capacity and concentrated transmission among devices to diminish the interference, even in congested environments. The traditional employment for this technology, can be summarised as follows:

i. Smart mobile phones, laptops, projectors, and tablets can all be docked wirelessly. ii. Many ultra-high definition videos and movies can be streamed at the same time.

iii. The WiGig technology permits users to download the HD videos fastly. iv. Enterprise bandwidth-intensive applications can be handled more easily.

c) **Automotive Applications:** Self-employment is a hot topic in the world of technology. It calls for detection in real-time and low latency of passengers and other obstructions. Accurate detection is important and decisions are necessary for the milliseconds. The best option for automotive radar detection is mm-waves.

d) **Short-range communications:** The 60GHz frequency band can be utilised for the shortrange communication such the personal networks, indoor applications, and point to point communications between two or more earth stations.

1.4 LITERATURE SURVEY

Many kinds of research and investigations have been conducted to study the 60 GHz frequency band, as well as to improve the performance of the antennas operating within it. Some of these studies can be summarised as follows:

a) In this article, the authors presented and discussed a novel of a small MPA design for unlicensed 60GHz mm-wave band employment. The simulated MPA is comprised of a rectangular radiated patch with it engraved a U-shape slot for the performance enhancement purpose, and powered via coaxial probe feed. The patch dimensions, feed point location, and U-slot dimensions have been subjected to a variety of parametric investigations. In addition, the simulated MPA and the antenna have been optimised to obtain the best possible results. The simulated MPA arrangement produced a wide BW of about 15.4GHz (25.69 %) comprising the frequency in the range of 52.20- 67.70GHz. The lowest return loss (S11) of the MPA is achieved to be equals to (–41.2dB) and the most gain is achieved to be equals to (9.52dBi) at the 60GHz operating frequency [11].

b) An approach for improving the antenna gain, (BW), and efficiency have been proposed by authors to respectively equal, 14dBi, 12.84%, and 94%. To develop manufacturing toleration, the simulated MPA was produced using the patch size enhancement procedure. The destine prototypes were manufactured using the low-cost printed circuit board turn technique and examined the frequencies in the X-band about 8-12GHz and the 60GHz band 57-66GHz. The gross performance of the MPA was preserved over the entire frequency range in which they are used. The IEEE 802.11ad and the IEEE 802.15.3c standard recommend that the MPA for the 60 GHz band satisfy the specifications for many Gb/sec data rate wireless local area networks and wireless personal area networks applications [12].

c) In this paper, the authors have been introduced a wide-bandwidth aperture-coupled MPA feeds through substrate combined waveguide technology for the V-band (i.e. 60GHz) to improve the whole antenna efficiency. The designed MPA have been utilised two distinct slot arrangements with a simulated impedance BW of 22% and an antenna gain of about 6.8dBi. Besides, the MPA presents wide BW characteristics [13].

d) In this article, the authors have been proposed a small compact twin-frequency band for 38 and 60GHzMPA with a unique design was intended for the 5G mobile handsets to link complex radiation parameters for twin-band performance. The simulated MPA is comprised of two electromagnetically joined patches. The first one is immediately feeds by a microstrip line and is essentially accountable for radiation in the lower band 38GHz. The next patch was feeding within both capacitive and inductive coupling to the primary patch and is essentially accountable for the radiation in the upper-frequency band (i.e. 60GHz). The mathematical and empirical obtained results show good performance concerning to the S_{11}, BW, and radiation patterns, efficiency, and antenna gain. The impedance matching BW achieved in the 38GHz and 60GHz bands are around the 2GHz and 3.2GHz, respectively [14].

e) This work illustrated an aperture-coupled MPA array based on the ridge gap waveguide feeding layer for the 60GHz applications. The innovation of this antenna can be summarised by the combination of comparatively modern gap waveguide technique forward with standard MPA arrays permitting to obtain the wideband characteristic amidst reasonable gain and moderate antenna efficiency. The researchers have been proposed n 8×8 element array, manufactured, and examined. The measuring results confirm the BW at a VSWR of 2 is around 15.5% (i.e. 57.5-67.2 GHz). In addition, about 75% antenna efficiency and greater than 21.5dBi antenna gain were achieved over operational BW. The achieved results for the proposed antenna were important for the valuation of the wideband planar MPA arrays within the mm-wave frequencies [15].

f) In this article, the authors have been proposed an MPA structure which able to overcome the surface waves stir that are produced due to the stout substrate in the MPA design by utilising the mushroom-like EBG (Electromagnetic Band Gap). Like the mentioned arrangement improve the MPA parameters such as the antenna gain, directivity, BW, and the efficiency. The authors have been determined the frequency band gap characteristics of the mushroom-like EBG unit cell value through utilising the CST package for the antenna simulation. The proposed MPA structure was stimulated for the 6GHz application [16].

1.5 PROBLEM STATEMENT

With a noticeable increase in applications that use wireless communications, there is congestion due to this abundance. In addition to the developments in the field of wireless communications, users are now aspiring to obtain high data transfer speeds, which can be obtained through the use of high frequencies around 60 GHz. One of the most important issues that should be taken in the seeing and seriously is the design of a small-sized antenna with satisfactory parameters. One of the most important issues that characterised the MPA is their narrow bandwidth and poor gain, so an adjustment and improvement must be made to overcome such issues.

1.6 THESIS OBJECTIVES

Many objectives comprise this thesis, which can be summarised as follows:

a) Design, simulation, and optimisation of rectangular MPA with an operated frequency band of 60GHz based on the finite integration technique that present in the Computer Simulation Technology (CST).
b) Enhancing the proposed antenna parameters by utilising the mushroom-like EBG structure.
c) Enhancing the proposed antenna parameters by utilising the passive Frequency Selective Surface (FSS) structure.
d) Compare the obtained results from the mushroom-like EBG with the results obtained from FSS.

1.7 THESIS OUTLINE

This thesis comprises of four chapters, the arrangements of the chapters in this thesis can be summarised as follows:

a) **Chapter Two:** This chapter of the thesis explains the fundamental antenna parameters such as radiation pattern, directivity, antenna gain, bandwidth, antenna equivalent circuit, and efficiency. Also, this chapter comprises a clarification about the MPA, MPA feeding techniques, Mushroom-like EBG, and FSS structure.

b) **Chapter Three:** This chapter of the thesis presents the basic and fundamental steps of the proposed antenna design. Also, in this chapter, the results obtained after conducting the simulation process by the CST software for the proposed designs of the antennas such as S_{11}, BW, and antenna gain will be presented.

c) **Chapter Four:** This chapter of the thesis presents the conclusion from this study and the advice through which could be developed for the proposed antennas in the future.

2. ANTENNA FUNDAMENTAL PARAMETERS

2.1 INTRODUCTION

In this chapter of the thesis, the fundamental antenna parameters such as radiation pattern, directivity, antenna gain, bandwidth, antenna equivalent circuit, and efficiency will be briefly presented as well as discussed. Also, this chapter comprises a clarification about the MPA, MPA feeding techniques, Mushroom-like EBG, and FSS structure.

2.2 ANTENNA PARAMETERS

Antenna parameters are fundamental and important matters for selecting and using antennas in virtually all disciplines. This chapter presents the necessary parameters of the antenna such as return loss (S_{11}), radiation pattern, gain, antenna equivalent circuit.

2.2.1 Antenna S_{11}

The antenna $S_{11}$is a significant term popular to utilise frequently in RF applications wherever the impedance matching is a decisive matter. The relationship of the power amount that is reflected from the antenna terminals because un-identical of the impedance among the antenna and source (i.e. impedance mismatching). The S_{11}can be defined as the loss of power within the signal that is returned/reflected by a discontinuity in a transmission line or the impedance mismatching. Ordinarily, decibels (dB) are utilised to express the S_{11}. In other words, if all of the power was directed to the load (e.g. antenna), the S_{11} would be limitless because the reflected power is close to zero. During antenna design procedure or the verification (i.e. testing practically), it is essential to measure the S11 and should be kept minimum as possible. Without minimum S_{11}, an antenna cannot convert the electrical wave into a radiated wave [18]. In general, the S_{11} can be expressed as follows:

$$S11 = 10 \log \left(\frac{P_f}{P_r} \right) \tag{2.1}$$

Where:

P_f: Is the forward power transmitted to the antenna;

P_r: Is the reflected power to the source.

2.2.2 Antenna Bandwidth (BW)

The BW of an antenna refers to the range of frequencies over which the antenna can operate correctly. The signal transition or signal receiving has occurred over a range of frequencies. This particular range of frequencies is allotted to a particular signal, so that other signals may not interfere in its transmission. BW is the band of frequencies between the higher and lower frequency over which a signal is transmitted, the defined BW is not used by others. The percentage ratio of the bandwidth is determined to know how much frequency variation either a component or a system can handle [19]. And it is calculated in terms of the percentage of the centre frequency of the band as presented in the following equation:

$$Bandwidth = 100 \times \frac{F_H - F_L}{F_C} \tag{2.2}$$

Where:

F_H: Is the upper operating frequency;

F_L: Is the lower operating frequency;

F_C: Is the centre frequency.

2.2.3 Antenna Directivity

The directivity of the antenna can be interpreted as the proportion of the radiation intensity of the antenna in a fixed direction away from the antenna to that are averaged in the whole rest directions. The mean radiation intensity is similar to the entire power radiated by the antenna divided on a 4π. If the direction isn't surely designated, the direction of the highest radiation intensity is implied [20]. Particularly, the directivity (*D*) of a non-isotropic source is equivalent to the attribution of its radiation intensity in a fixed direction on that of the isotropic exporter, as follows:

$$D = \frac{U}{Uo} \tag{2.3}$$

If the direction isn't designated, it signifies the direction of highest radiation intensity (i.e. maxi *D*) can be determined as follows:

$$D = \frac{U_{max}}{U_o} = \frac{4\pi U_{max}}{P_{rad}} \tag{2.4}$$

Where:

U_{max}: Is referring to the highest directivity of the antenna;

U_o: Is referring to the isotropic source radiation intensity;

To epitomise the D definition, the D of the antenna is the measure that explains the directional characteristics of the antenna, and it is consequently controlled simply by the pattern.

2.2.4 Antenna Gain

It is realized as the capability of the antenna to radiate more or less in any direction compared to an isotropic antenna. If an antenna could be made as a perfect sphere, it would radiate equally in all directions. Antenna gain is linked to the directivity of the antenna, as the directivity is known by how much an antenna focused the energy in certain direction in preference to radiation in other directions. So, if we consider that an antenna is 100% efficient, then the directivity would be equal to the antenna gain and the antenna would be an isotropic radiator. Hence, the gain is equal to the amount of power that can be achieved in one direction at the expense of the power lost in the others [21]. The gain is continuously related to the most lobe and is indicated in the direction of greatest radiation unless indicated, antenna gain can be expressed by:

$$G(\theta,\emptyset) = e.D(\theta,\emptyset) \quad (dBi) \tag{2.5}$$

Where:

$G(\theta,\emptyset)$: Is referred to the antenna gain;

$D(\theta,\emptyset)$: Is referred to the antenna directivity;

e: Is the antenna efficiency.

2.2.5 Radiation Pattern

An antenna radiation pattern or more practically "antenna pattern" is can be defined as the mathematical relation or a graphical illustration of the radiation features of the antenna as an action of space coordinates. It illustrates how the antenna guides the energy radiates and it is calculated in the far-field zone. Figure 2.1, displays the general radiation pattern for the directional antenna. The pattern of the antenna comprises a principal lobe and some secondary or more practically called minor lobes. All kinds of the antennas, excluding the monopoles and dipoles, the sidelobe as well as the back lobes could be achieved but they are often unsatisfactory this due to the waste the energy for transmitting antennas and inherent noise sources for receiving antennas [22].

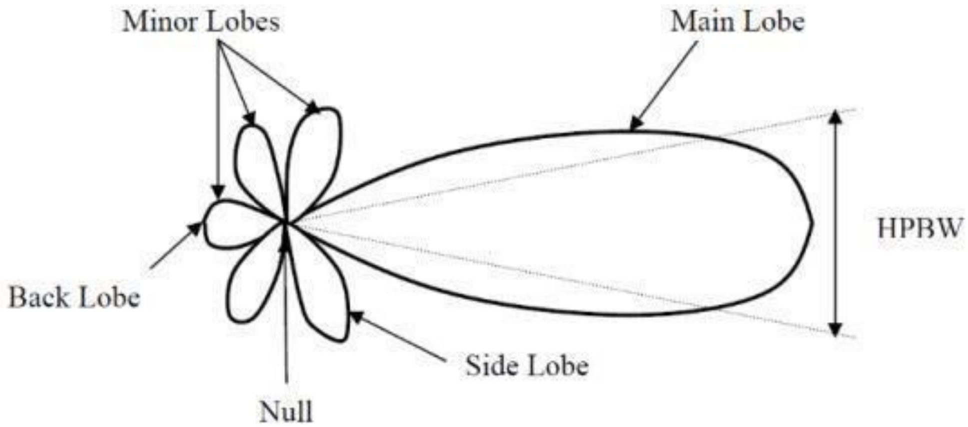

Figure 2.1: General organisation of the radiation pattern for a universal antenna.

2.2.6 Antenna Equivalent Circuit

The input impedance of the antenna is characterised as the impedance displayed by an antenna at its terminals or the ratio of the voltage to the current at the combine of terminals or the ratio of the fitting components of the electric to magnetic fields at a point. Subsequently, the impedance of the antenna can be composed as:

$$Z_{in} = R_{in} + jX_{in} \tag{2.6}$$

Where:

Z_{in} : Is indicating to the antenna impedance at the terminals;

R_{in}: Is indicating to the antenna resistance at the its terminal;

X_{in}: Is indicating the antenna reactance at the terminals.

The antenna impedance comprises of two parts the first part is the real part which shows the power dissipated as radiation while the second part is the imaginary part which dissipates the power as a loss, this due to the nature of the material that is made up of the antenna, Figure 2.2 illustrates the equivalent circuit that represents the antenna in the impedance form [22].

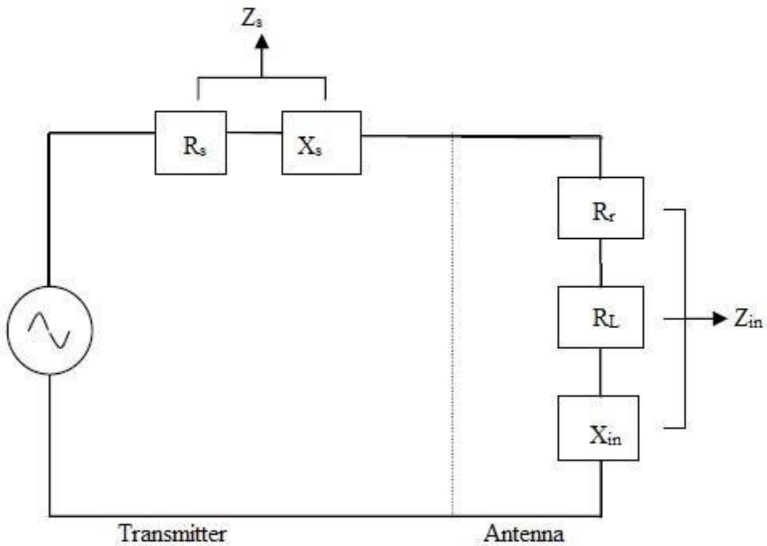

Figure 2.2: Antenna equivalent circuit.

2.3 MICROSTRIP ANTENNAS

The microstrip antennas have a widely present-day development. This type of antennas was designed to be helpful in the integration with the other driving circuitry of the communication system on a commonly printed circuit board or a semiconductor chip. Other than other coming about focal points, the integrated-circuit innovation for the antenna manufacture permitted high dimensional precision, which was something else troublesome to attain in conventional creation methods. In general, such antenna structure is consist of dielectric material commonly called substrate with a height (d) and dielectric constant (ε_r) as well as a metallic material printed on the face of the substrate or both of the face and the bottom depending on the antenna type.

2.3.1 The MPA

In the wireless communication tools and systems, the MPA is usually utilised which is fabricated utilising the photolithographic procedures for the printed circuit board. The geometry of the MPA antenna comprises of a dielectric substrate of a certain thickness (d), having a total metalisation on one of its bottom and of a metal “patch” on the other side (i.e. its face). The substrate of the MPA is usually thin ($d \ll \lambda$). The metal patch on the front surface can have different shapes, in spite of the fact that a rectangular shape, as appeared in Figure 2.3, is commonly used [24].

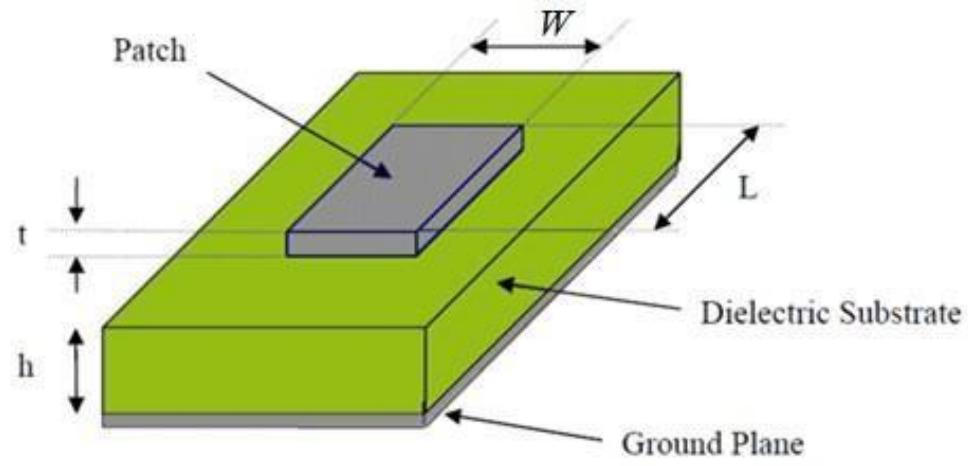

Figure 2.3: Structure of the rectangular MPA.

The antenna may be energised by utilising different strategies. One common approach is to feed on a microstrip line (see Figure 2.4); connecting the microstrip antenna at the centre of one of its edges. The microstrip line may be associated with a feeding circuitry or specifically fed by interfacing a flag source over the microstrip line and the ground plane.

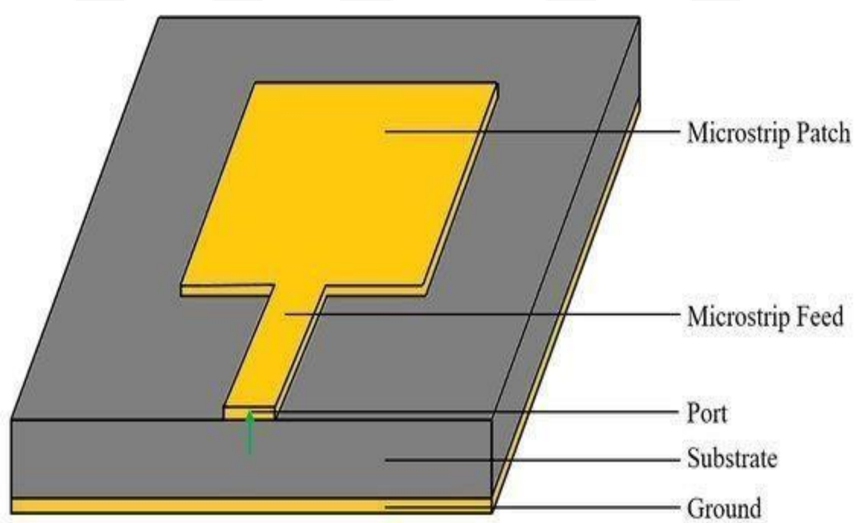

Figure 2.4: Structure of the rectangular MPA with microstrip feed line.

The MPA produces the most extreme radiation within the broadside course and ideally no radiation within the end-fire course. The measure of the antenna is usually outlined such that the antenna resounds at the working frequency, creating a genuine input impedance. For a rectangular MPA, this requires the length of the antenna, L_p, to be approximately half a wavelength within the dielectric medium. The width of the antenna, W_p, on the other hand, determines the level of the

input impedance. The microstrip antenna can be thought of as a rectangular cavity with open sidewalls. The fringing fields through the open sidewalls are responsible for the radiation. However, the structure is principally a resonant cavity, with only limited fringing radiation.
Therefore, the bandwidth of the radiation is poor compared to the bandwidth of the other antennas.

2.4 FEEDING TECHNIQUES FOR MPA

There are many methods that can be utilised for feeding the MPA. These methods can be categorised into conducting techniques such as the line feed and the coaxial feed. While another category is the non-conducting methods such as proximity and aperture coupling. All of the mentioned methods will be presented and clarified in the next subsections [25], [26].

2.4.1 Microstrip Line Feed

In this sort of the feeding procedure, a conductive stripe (i.e. line) is associated immediately to the end of the radiated patch as appeared in Figure 2.4. The conductive stripe is littler in width in the comparison to the patch; such sort of the feeding strategy offered the utility that summarized as the feeding is be carved on the corresponding substrate with the patch to produce the planar structure. On the other hand, the main drawback of this feeding method is the additional radiation from the line which is affecting on the total antenna radiation pattern.

2.4.2 Coaxial Feed

The Coaxial feed or most popularly as probe feed could be an exceptionally common procedure employed for bolstering the MPA performance by eliminating the presence of the external radiation from the line feed. As illustrated in Figure 2.5, the internal core of the coax connector expands out of the substrate of the MPA and is cemented with the patch, whereas the external (i.e. second conductor of the coax) conductor is associated with the MPA ground plane. The most utility of the using of such sort of the feeding method is that the coax position could be put at any craved area interior the patch in arrange as the required impedance matching. This feeding strategy is easy to manufacture as compared to the other methods and hasn't extra radiation due to the absent of the feeding line. In any case, its principal drawback can be summarised as it gives a limit bandwidth and is troublesome to show since the gap needs to made within the substrate and the connector projects exterior the ground plane, in this way doesn’t making the MPA totally planar in the case of the thick substrates ($h > 0.02\lambda o$). Moreover, for thicker substrates, the expanded plumb-line length makes the input impedance extra inductive, driving to coordinating issues.

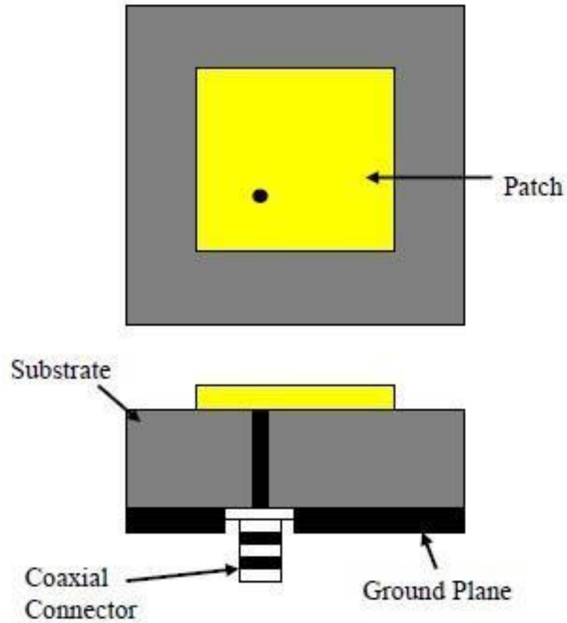

Figure 2.5: Rectangular MPA with probe feed.

2.4.3 Aperture Coupled Feeding

In this sort of the feeding procedure, there is a metal ground plane organised in order to split the patch of the antenna from the feed line, as presented in Figure 2.6As the conjunction amidst the patch and the feeding line is performed out of a small space (i.e. gap) engraved on the utilised ground plane.

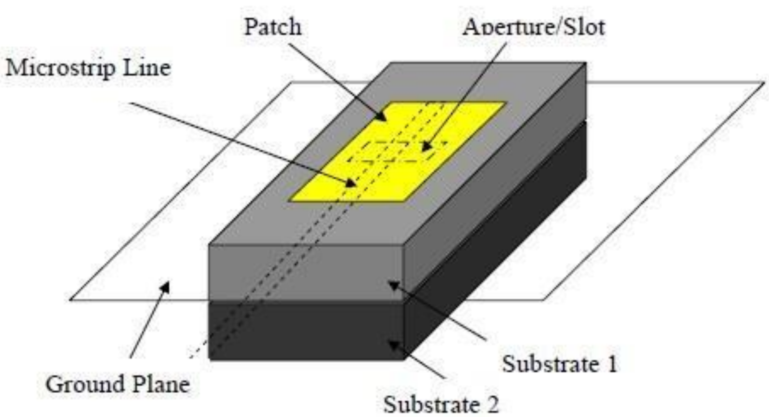

Figure 2.6: Rectangular MPA with aperture coupled feed.

The coupling gap is more often than not centred beneath the fix, driving to minify crosspolarisation this because of the structure symmetry. In order to control the amount of the coupling, the gap shape and size is modified. Considering the utilised ground plane is isolating the patch and the feeding line, the extra radiation of feed is depreciated. By and large, because a use of a two distinct substrates, the antenna thickness will have risen contributes to the manufacturing difficulties, this issue defecting this feeding method although it's offered many of the benefits.

2.4.4 Proximity Coupled Feeding

This sort of the feeding strategy is additionally named as the electromagnetic coupled method. As appeared in Figure 2.7, there are a two dielectric substrates are utilised and the feed line is situated as a sandwich among them and the transmitting patch is on the rested over the upstairs substrate. The most merit that characterised this strategy is that it dispenses with additional radiation that emitted from the metal feed and gives exceptionally tall bandwidth (as high as 13%), due to in general increment within the total thickness of the MPA. This conspires to gives opportunities among two of the diverse dielectric media, one for the patch and further for the feed line to optimising the person exhibitions.

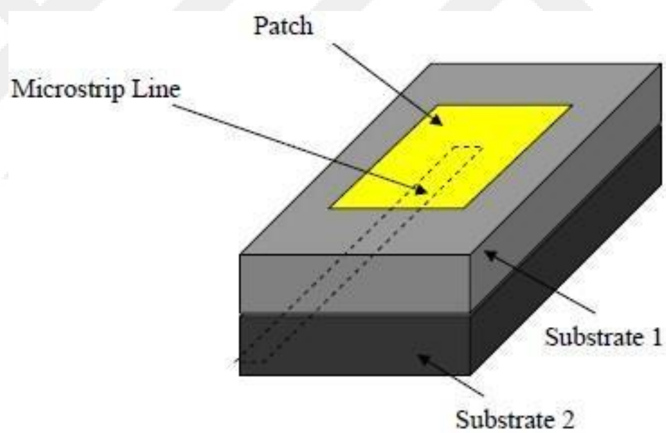

Figure 2.7: Rectangular MPA with the proximity coupling feed.

2.5 RECTANGULAR MPA DESIGN

In order to design the rectangular MPA, the transmission line model for the MPA analysis can be utilised. This method realises the MPA with two identical slots with a width of (W) and a thickness of (h), divided by a transmission line with a length of (L). The microstrip line is actually a nonhomogeneous line of a pair of the dielectrics, normally the substrate and the air, as presented in Figure 2.8.

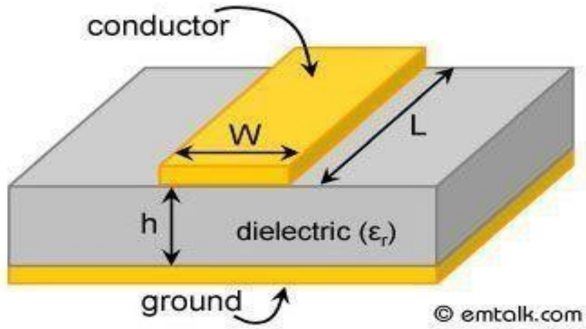

Figure 2.8: Representation of the MPA.

Therefore, as confirmed from Figure 2.9, the greatest of the electric field lines remain in the substrate and portions of some lines in the air. As a result, this transmission line can't support the true transverse electric magnetic mode of transmission, considering the phase velocities would be distinctive in the air and the substrate [22].

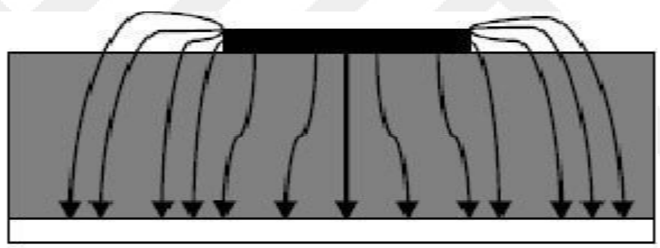

Figure 2.9: The electric field lines.

Alternatively, the predominant mode of the spread would be the quasi-TEM mode. Therefore, an effective dielectric constant ($\varepsilon_{r_{eff}}$) necessity be obtained to estimate for the fringing and the wave spread in the line. The value of the $\varepsilon_{r_{eff}}$ is lightly smaller than that of the ε_r, this because the effect of the fringing fields round the perimeter of the patch of the MPA isn't restricted in the substrate but is further propagated in the air as mentioned previously in Figure 2.9. In order to obtain $\varepsilon_{r_{eff}}$ mathematically, the following equation can be applied:

$$\varepsilon_{reff} = \frac{\varepsilon_r + 1}{2} + \frac{\varepsilon_r - 1}{2}\left[1 + \frac{12h}{W}\right]^{-.05} \tag{2.7}$$

The fringing lines over the width can be represented as radiating slots so that in an electrical manner the patch of the MPA seems to be greater than its substantial size. From this can conclude that the dimensions of the patch over its length are expanded for each end by a factor called ΔL, which can be calculated by applying the following equation:

$$\Delta L = 0.412h\frac{\left(\varepsilon_{reff} + 0.3\right)\left[\frac{W}{h} + 0.264\right]}{\left(\varepsilon_{reff} - 0.258\right)\left[\frac{W}{h} + 0.8\right]} \qquad (2.8)$$

Presently, the exact length (i.e. effective) of the patch can be calculated mathematically by applying the following equation:

$$L_{eff} = \frac{c}{2f_r\sqrt{\varepsilon_{reff}}} \qquad (2.9)$$

$$L = L_{eff} - 2\Delta L \qquad (2.10)$$

Every of the previously mentioned radiating slot could be served as an analogous equivalent admittance Y, as shown in Figure 2.10, each slots are named as S_1 and S_2, respectively.

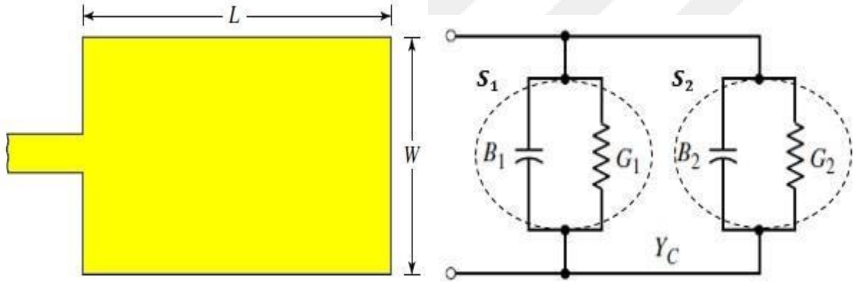

(a) Rectangular shape patch. (b) Equivalent circuit.

Figure 2.10: Rectangular microstrip patch with its equivalent circuit.

The tantamount admittance of S_1, can be represented as follows:

$$Y_1 = G_1 + jB_1 \qquad (2.11)$$

$$G_1 = \frac{W}{120\lambda_o}\left[1 - \frac{1}{24}(K_o h)^2\right] \qquad \frac{h}{\lambda_o} < 0.1 \qquad (2.12)$$

$$B_1 = \frac{W}{120\lambda_o}\left[1 - 0.363\ \ln(K_o h)\right] \qquad \frac{h}{\lambda_o} < 0.1 \qquad (2.13)$$

Considering the S_2 is analogous to the S_1, so its tantamount admittance can be expressed as follows:

$$Y_2 = Y_1, \quad G_2 = G_1, \quad B_2 = B_1$$

(2.14)

The totally admittance of the S_1 (i.e. input admittance) is found by transforming the admittance of the S_2 from its output terminals to the input terminals utilising the admittance transformation formula, hence the transformed S_2 now represented as follows:

$$\tilde{Y}_2 = \tilde{G}_2 + j\tilde{B}_2 = G_1 - jB_1 \qquad (2.15)$$

Thus, the totally resonant input admittance is real quantity, which can be represented as follows:

$$Y_{in} = Y_1 + \tilde{Y}_2 = 2G_1 \qquad (2.16)$$

The totally input impedance can be represented as follows:

$$Z_{in} = \frac{1}{Y_{in}} = R_{in} = \frac{1}{2G_1} \qquad (2.17)$$

Considering the resonant input resistance is provided by the previously mentioned equation (2.17) don't taking the mutual influence amidst the S_1 and the S_2. Consequently, necessary to adjust the previous equation (2.17) to be represented as follows:

$$R_{in} = \frac{1}{2(G_1 \pm G_{12})} \qquad (2.18)$$

Whereas the plus (+) is utilised to specify the modes with odd (i.e. anti-symmetric) resonant voltage distribution beneath the patch and among the slots. However the minus (−) is utilised for the mode with the even (i.e. symmetric) resonant voltage distribution. The G_{12} can be calculated from the following equation:

$$G_{12} = \frac{\quad}{\quad^{2}} \quad 1 \quad \pi \quad \sin\left(\frac{k_o W}{2} \times \cos(\theta)\right)^{2} \quad 3 \qquad (2.19)$$

Where J_o is the Bessel function of the 1st kind of the order of the zero. For the usual MPA, the R_{in} is obtained from equation (2.18), is indicated at the S_1. Nevertheless, it has been presents that the resonant input resistance could be varied through utilising the inset feed within the patch, via a distance f_i from the S_1, as presented clearly in Figure 2.11. This manner can be utilised effectively to obtain the best match between the patch antennas by using a microstrip-line.

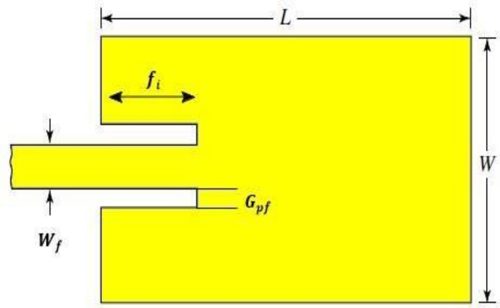

Figure 2.11: Rectangular patch with inset feed line.

The characteristic impedance of the feed line that utilised to powering the MPA can be obtained by applying the following equation:

$$Z_C = \Big\{ \qquad 120\pi \qquad W_f \tag{2.20}$$

Where the W_f referred to the width of the microstrip feed line and the input resistance of the inset feed can be displayed as follows:

$$R_{in}(y = y_o) = R_{in}(y = 0)cos^2\left(\frac{\pi}{L}\, f_i\right) \tag{2.21}$$

Where:

R_{in} : is the referred to equivalent input impedance at the edge of the antenna radiating patch; Z

: is referred to the equivalent feed line impedance usually chosen as 50 Ω.

The width of the feed line is obtained mathematically by utilising the following equation:

$$W_f = \frac{2h}{\pi}\left\{B - 1 - \ln(2B - 1) + \frac{\varepsilon_r - 1}{2\varepsilon_r}\left[\ln(B - 1) + 0.39 - \left(\frac{0.61}{\varepsilon_r}\right)\right]\right\} \tag{2.22}$$

$$B = \frac{377\pi}{2Z_0\sqrt{\varepsilon_r}}, \tag{2.23}$$

2.6 FREQUENCY SELECTIVE SURFACE (FSS) AND APPLICATIONS

The FSS is a planar periodical structure that exhibits reversal or transmission characteristics as a function of the operating frequency. The surface comprises tender conducting components, ordinarily engraved on dielectric material commonly named as a substrate. These structures function as electromagnetic filters usually categorised as passive, selectively reversing, or attenuate the coveted frequency band. This selectivity appears from the periodicity that the conducting components have among each other [27]. According to the component geometry, the FSS have many employments, which can be summarised as follows:

- Low-Pass;
- High-Pass;
- Pass-Band, and
- Stop-Band Filter.

Figure 2.12 exhibits a standard model of the FSS that have the previously mentioned behaviour. The investigations of the periodical arrangements or the FSS didn't escalate till the year 1960, during their potential for military purposes were achieved, particularly in stealth technology.

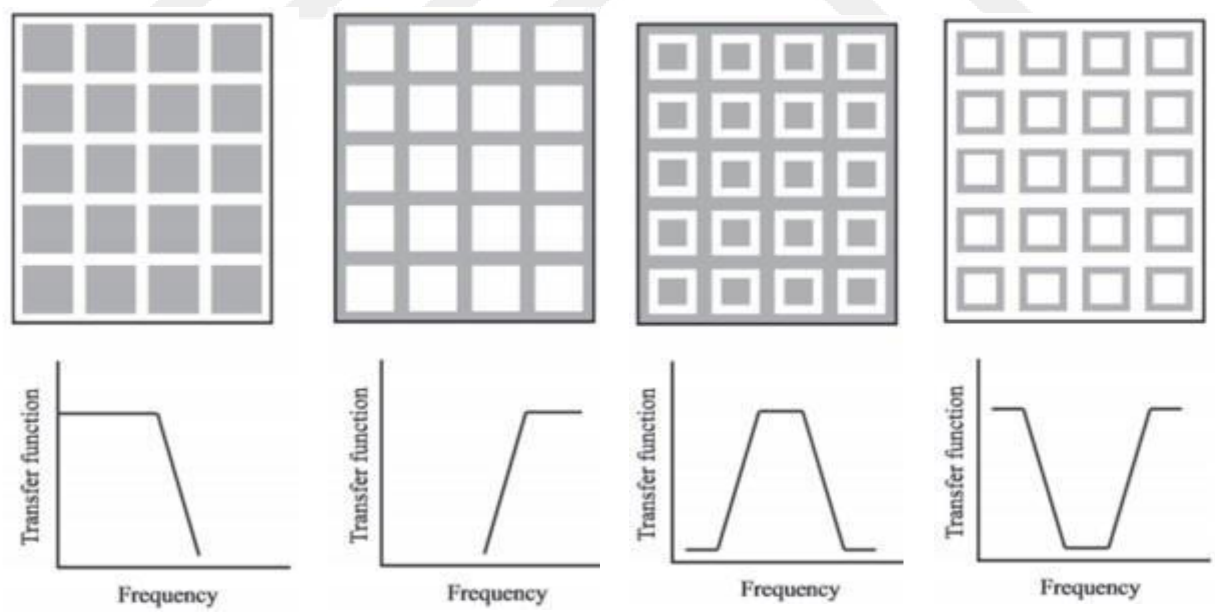

(a) $Low - pass$ (b) $High - pass$ (c) $Pass - band$ (d) $Stop - band$

Figure 2.12: The applications of the FSS in the filter modes.

Since the year 1960, the FSS was extensively employed in many of the applications such as the antenna, radar, and the satellite communications. An example, the FSS is commonly utilised as secondary reflectors in the Cassegrain scheme with the parabolic dish antenna, as depicted in

Figure 2.13-(a). Like these reflectors are seldom related to dichroic structures, which are sheer to a single frequency band ($f1$) however covered to the different frequency band ($f2$). An additional example on the FSS utilisation is in the antenna or for the electromagnetic absorber, as shown in Figure 2.13-(b). Repeatedly, the FSS reversal the undesired transmissions in the $f2$ while permitting the eligible transmissions in the $f1$ to cross through it. According to the form of the FSS, the transmitted signals that aren't in the operation band can be carefully reversal away in specific directions to diminish the radar cross-section of the antenna [28].

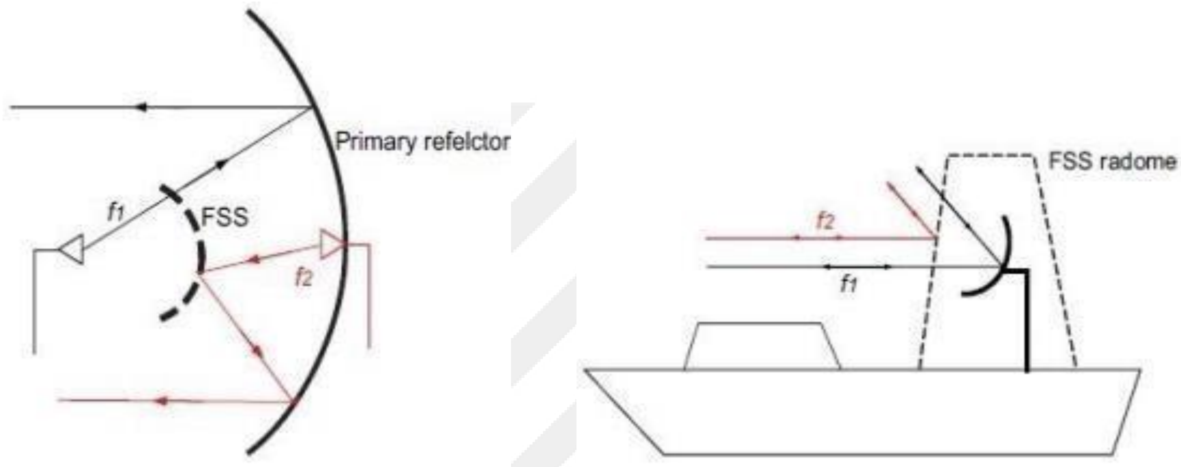

(a) FSS as secondary-reflector. (b) FSS the antenna dome.

Figure 2.13: Some of FSS applications.

An extra field of concern of the FSS utilisation is in the superstrate above/below the MPA to enhance their radiation components. Furthermore, the FSS has observed practice in other uses, apart from the utilisations in antenna design. For example, is their employment in the circuits of the analog absorbers in order to improve the wireless communication arrangements within the indoor environments. Utilising the FSS in the indoor environments to selectively manage the propagation of the waves like as the blocking of the mobile cell phone transmission into stockades, the cinemas, the hospitals, and the places of faith, or in the airport [29].

2.7 MUSHROOM LIKE ELECTROMAGNETIC BANDGAP (EBG)

In the antennas especially the MPA the surface waves don't radiate in the free space but it propagates straight to the ground plane, therefore, this is unwanted in the antenna design. This diminishes the performance of the MPA such as the efficiency, the gain, the directivity, and border bandwidth. In the case of the permittivity (i.e. dielectric constant) of the substrate is higher than

"1", this leads to the surface waves exciting on the MPA [30]. Additionally, to the end-fire radiation manner, the conjugation among diverse array components is further created via the surface waves. Such waves are inspired to the substrate of the antennas at the elevation angle (θ) resting among 0.5π and $sin^{-1}d\ (\frac{1}{\sqrt{\varepsilon_r}})$. Such waves are reversed from the ground plane of the antenna later being an occurrence about the corner that meets the dielectric-air interface as well as gets reversed from there. The surface waves arrive at the border of the MPA construction next to this zig-zag route, as illustrated in Figure 2.14- (a), whereas the end-fire radiation will be created due to their reflection and diffraction above the edges [31].

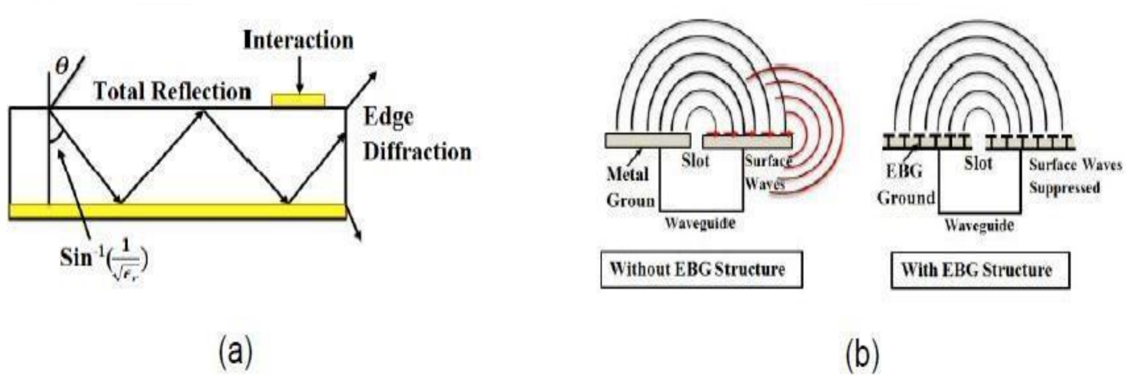

Figure 2.14: (a) Exterior wave propagation on the substrate, (b) propagation of the exterior waves utilizing the EBG structure.

Through the latest decades, multiple of technologies were improved to minimise the surface waves excited by the MPA. For example, installing an extra dielectric sheet on the top of the patch or optimising the patch configuration (i.e. modify the patch design). Digging a small air cavity beneath the patch to realise the depressed dielectric constant. As the dielectric constant rise, the exterior waves become more cumbersome, although the side influence for arranging this is the bandwidth decrease and this difficulty could be resolved by raising the height of the substrate. The procedure for practising the EBG is a proper means to overcome the exterior waves which occur from the large and thick permittivity of the substrate due to proposed the stop-band about the wanted frequency. A surface wave is the TM and TE forms of the substrate. Such two forms are characterised by "waves attenuating" in the transverse trend and having an extremely propagation constant over the cut-off frequency [32]. The phase velocity of the exterior waves is completely related to the substrate specifications (i.e d and ε_r). Figure 2.14-(b) illustrates the blocking of the propagation of the exterior (i.e. surface) wave on the waveguide through the utilising of the EBG construction. The EBG has been proposed based on the phenomena of the photonic bandgap in the optical field. The EBG periodical structure has been employed in the microwave planar waveguides that can contribute to pass or stop-bands. There are two varieties of the EBG constructions, the first type is popularly called the "mushroom" surface with the utilising of the vias, while the other type is the uni-planar EBG surface without utilising of the vias. The principal benefits of the mushroom-like EBG surface could be summarised by the accomplishment of a broad bandwidth. The characteristic of the surfacewaves elimination maintains the reducing of the reversed direction and the quantity of the power wasted leads to the enhancement in the MPA performance [33], [34].

3. ANTENNA DESIGN AND SIMULATION

3.1 INTRODUCTION

In this chapter of the thesis, the basic and fundamental steps of the proposed antenna design will be clarified as well as explained. Also, in this chapter, the results obtained after conducting the simulation process by the CST software for the mentioned antennas such as S_{11}, BW, and antenna gain will be presented.

3.2 ANTENNA DESIGN

In this section of the chapter the design process for the base rectangular MPA, rectangular MPA with the mushroom-like EBG, and rectangular MPA with the FSS substrate.

3.3 BASE RECTANGULAR MPA DESIGN

In order to design the base rectangular MPA, there are many parameters that should be considered which can be summarised as follows:

a) **Operating frequency band (f_r)**: The f_r for the MPA necessity to be selected relating with the required applications.
b) **The dielectric constant:** Each substrate has its own characteristic most important one is the ϵ_r, which always in the range of $2.2 \leq \epsilon_r \leq 12$.
c) **The height of dielectric**: For the MPA to be utilised in the up-to-date employments, it is necessary low profile. So that the h of the dielectric must be not exceed the range of $0.003\lambda_o \leq h \leq 0.05\lambda_o$.

The antenna base antenna is a rectangular MPA, its dimensions have been determined by utilising the equations of section (2.5) and by written a MATLAB code to facilitate the calculation and get accurate results as well. After that, the simulation procedure is launch using the CST software. It is necessary to mention that the primary parameters that were previously mentioned should be set as demonstrated in Table 3.1 for our study. The simulated base rectangular MPA in the CST software is presented in Figure 3.1. Whereas the size of the radiated patch, feed line, and distance between them is shown in Figure 3.2.

Table 3.1: Essential parameters values.

Parameter	Value
f_r	60GHz
ε_r	2.2
h	0.1mm

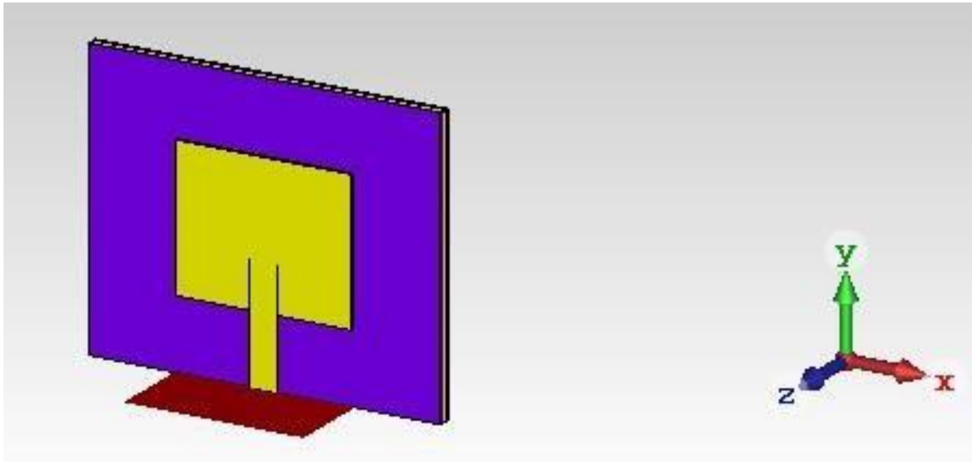

Figure 3.1: Base rectangular MPA in the simulation software.

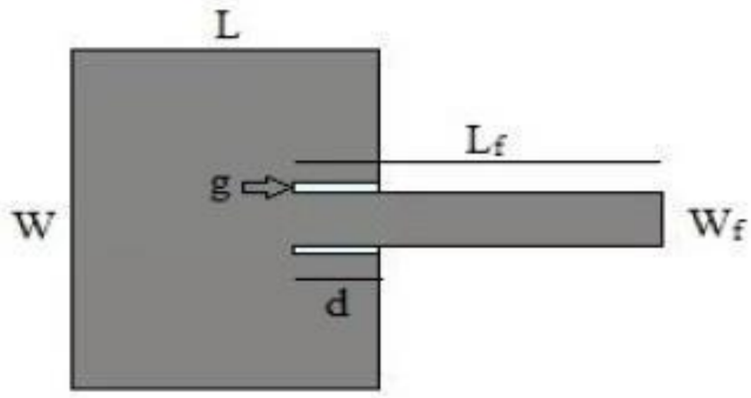

Figure 3.2: Organisation of patch and feeding line.

In this study, to boost up the simulation operation and get the required results the Optimisation procedure has been applied. In our work, the trial/error optimisation scheme was utilised by minimising or maximising the antenna dimensions unto reaching the required results. Following doing sundry tries of the dimensions trial/error optimisation scheme, Table 3.2 demonstrate the final dimensions for the base rectangular MPA and Figure 3.3 shows the optimised base rectangular MPA in the software of the simulation. Following doing sundry tries of the dimensions trial/error optimisation scheme, Table 3.2 demonstrate the final dimensions for the base rectangular MPA and Figure 3.3 shows the optimised base rectangular MPA in the software of the simulation.

Table 3.2: Calculated and optimised dimensions for the base rectangular MPA.

Parameter	Calculated (mm)	Optimised (mm)

W	1.975	2.0
L	1.6301	1.63
fi	0.5564	0.532
W_f	0.308	0.305
L_f	1.8263	1.826
g_{pf}	0.0179	0.1

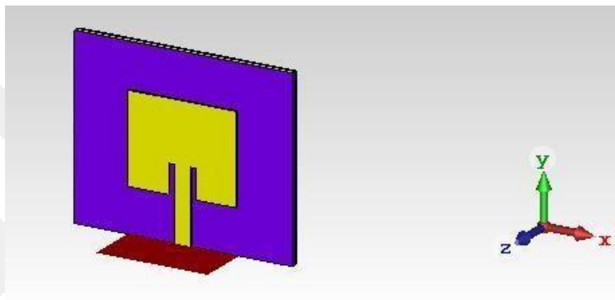

Figure 3.3: Optimised base rectangular MPA.

3.4 SIMULATIONS RESULTS FOR THE BASE RECTANGULAR MPA

In this section of this chapter of the thesis the accomplished results for the base rectangular MPA like the gain, return loss S_{11}, and bandwidth will be displayed and explained.

3.4.1 The S_{11} results

The S_{11} of the MPA represents the reflex of signal power from the MPA terminals relative to the transmitted signal power from the source. Consequently, it is necessary to maintain its value a minimum as possible. The antenna designer suggests testing the antenna at $S_{11} = -9.5dB$ which means that just a 10% of the transmitted power does reflex back toward the source whilst the outstanding of 90% is reached to the antenna successfully. The acquired S_{11} for the base rectangular MPA is reached with some shifting at $59.96GHz$ and equals - $7.59dB$, as illustrated in Figure 3.4.

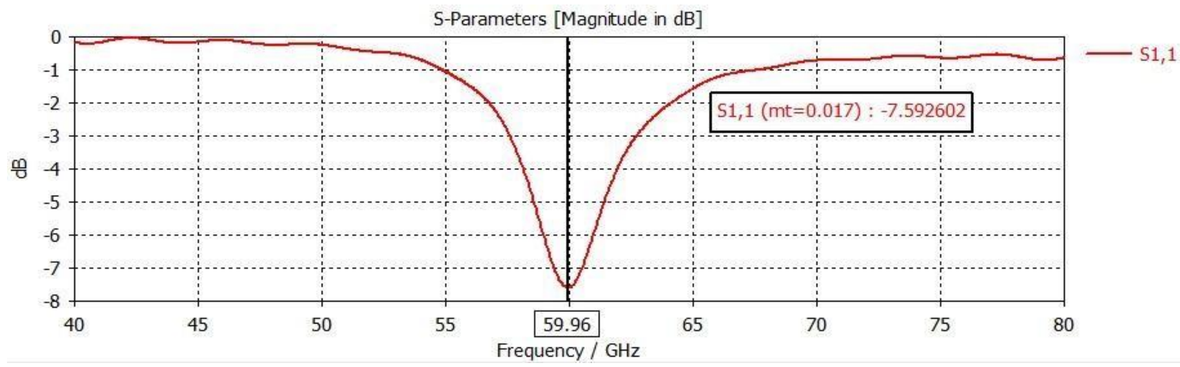

Figure 3.4: The S_{11} for the base rectangular MPA.

This value meaning there is a big mismatching between the source and the antenna. The required S_{11} should be at least $-9.5dB$ at $fr = 60GHz$. To resolve this problem some modifications to the antenna dimensions should be applied. In simile to the optimised MPA, the S_{11} after optimisation is better, as presented in Figure 3.5. The frequency was shifted to 59.32 GHz with -9.98 dB S_{11}, and at the required operating frequency (i.e. 60 GHz) the S_{11} enhanced to be -9.98 dB which is close to the acceptable range.

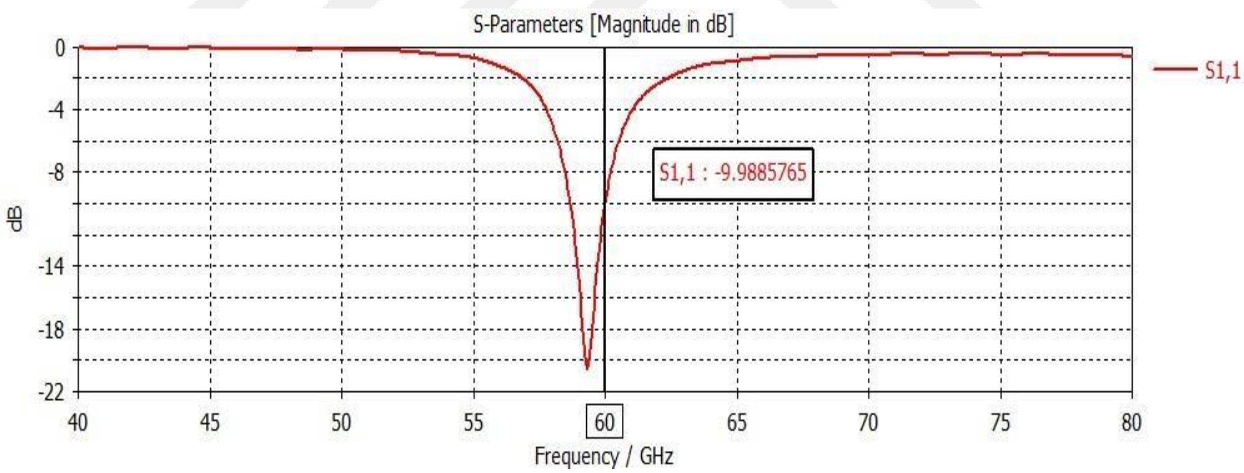

Figure 3.5: The S_{11} for the base rectangular MPA after the optimisation.

3.4.2 Antenna BW

The BW of any antenna could be obtained by using the S_{11} graph. The BW of the antenna can be acquainted as the range of frequencies in which the S_{11} of the antenna is equal to or smaller than the $-9.5dB$ [35]. The bandwidth of the base rectangular MPA is determined from theS_{11}, as presented below in Figure 3.6, to be $1248MHz$.

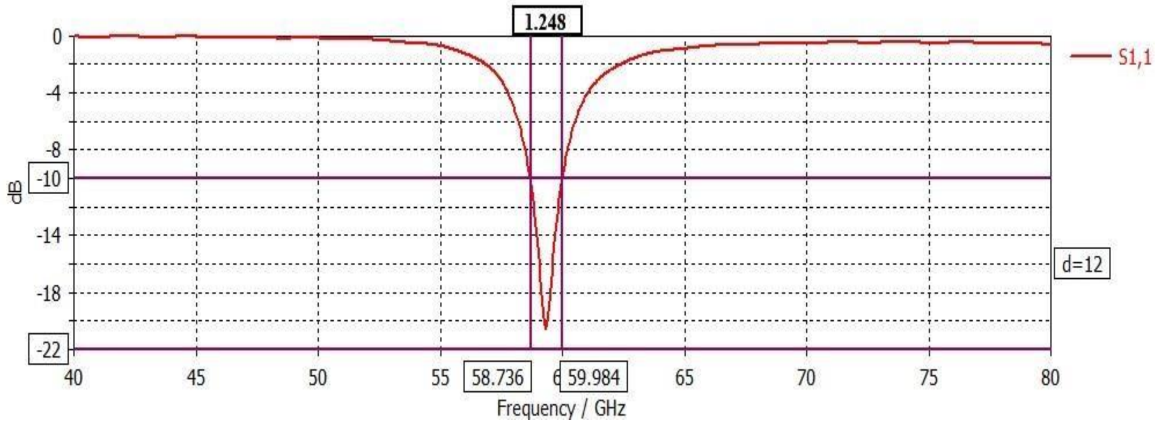

Figure 3.6: Optimised BW for the base rectangular MPA.

3.4.3 Antenna Gain

The MPA are famous for their bad gain; this is because antenna gain is influenced by the (h) and (ε_r) of the substrate [36]. For the base rectangular MPA, the gain is acquired to be 6.87dBi, as shown in Figure 3.7.

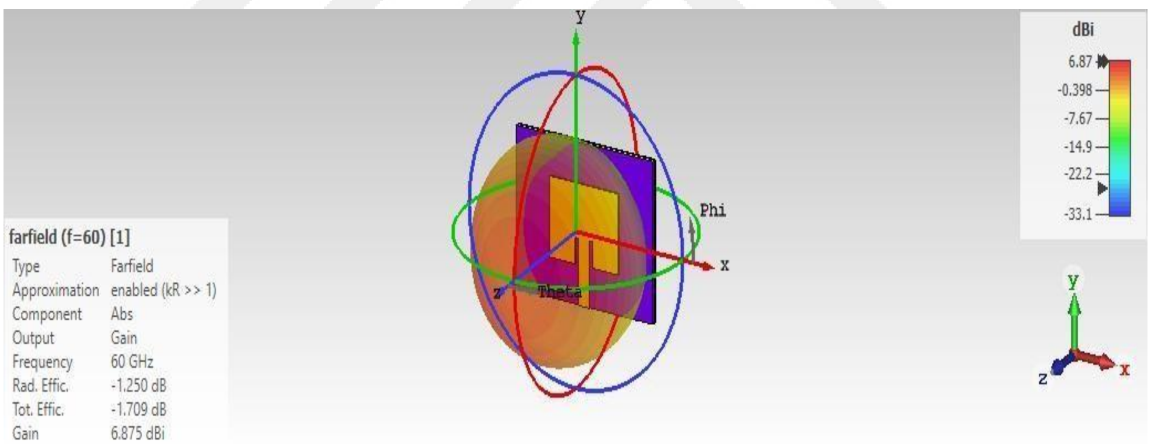

Figure 3.7: Optimised gain for the simulated rectangular MPA.

3.5 MUSHROOM ANTENNA DESIGN

The previous design of the base rectangular MPA was loaded with the mushroom-like EBG structure as illustrated in Figure 3.8. The dimensions of the mushroom-like EBG structure and the separation distance among the elements was obtained by utilizing the trial and error scheme until the best results reached. Table 3.3 presents the size and the separation among the element and antenna radiating patch as well.

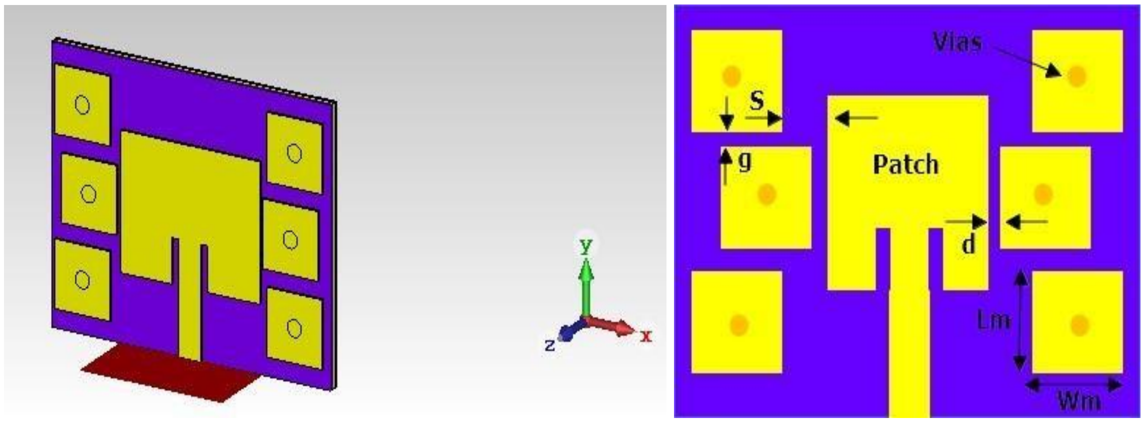

(a) (b)

Figure 3.8: Rectangular MPA surrounded by mushroom-like EBG structures; (a) Antenna inside CST software; (b) Dimensions of the mushroom-like EBG.

Table 3.3: Dimensions and spacing of the mushroom-like EBG parameters.

Parameter	Dimension (mm)
Mushroom-like EBG cell width (W_m)	0.8
Mushroom-like EBG cell length (L_m)	0.8
Gap between adjacent cells (g)	0.1
Distance between middle cell and patch (d)	0.05
Spacing between the edge cells and patch (S)	0.2

3.6 SIMULATION RESULTS FOR THE RECTANGULAR MPA WITH MUSHROOM LIKE EBG

This section exhibits the results for the S11, gain, and bandwidth for the rectangular MPA after adding the mushroom-like EBG structure.

3.6.1 The S_{11}

The S11 of the rectangular MPA with the mushroom-like EBG structure from CST software is presented in Figure 3.9. The S_{11} at 60GHz equals -29.77dB. In comparison to the mushroom loaded rectangular MPA, the return loss after adding the mushroom-like EBG structure is better.

The frequency was shifted to 60 GHz as the required and the mismatch problem was solved.

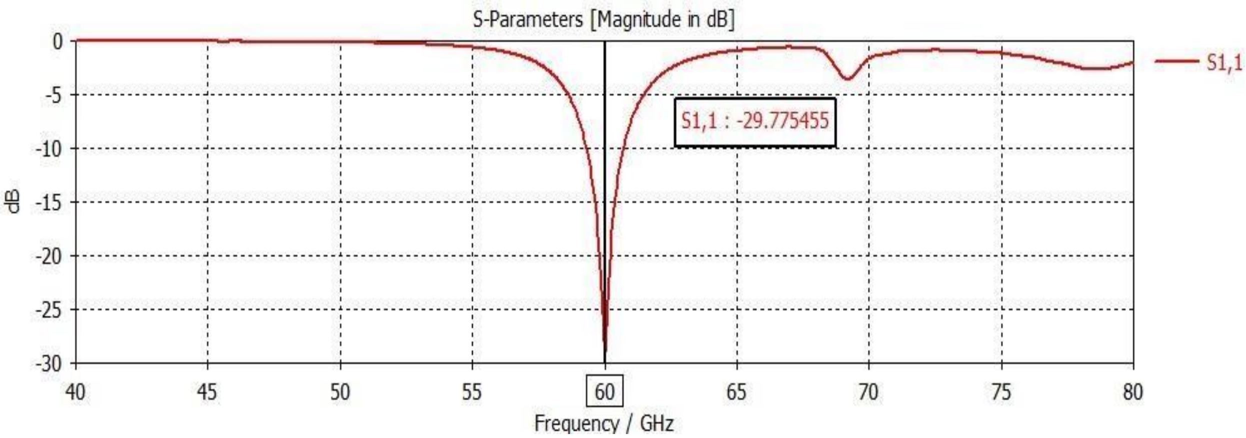

Figure 3.9: The S_{11} of the rectangular MPA with mushroom-like EBG.

3.6.2 Antenna BW

The BW of the rectangular MPA with the mushroom-like EBG structure is obtained from the return loss plot to be 1400.3 MHz, as exhibited in Figure 3.10 which is better than that of the base rectangular MPA.

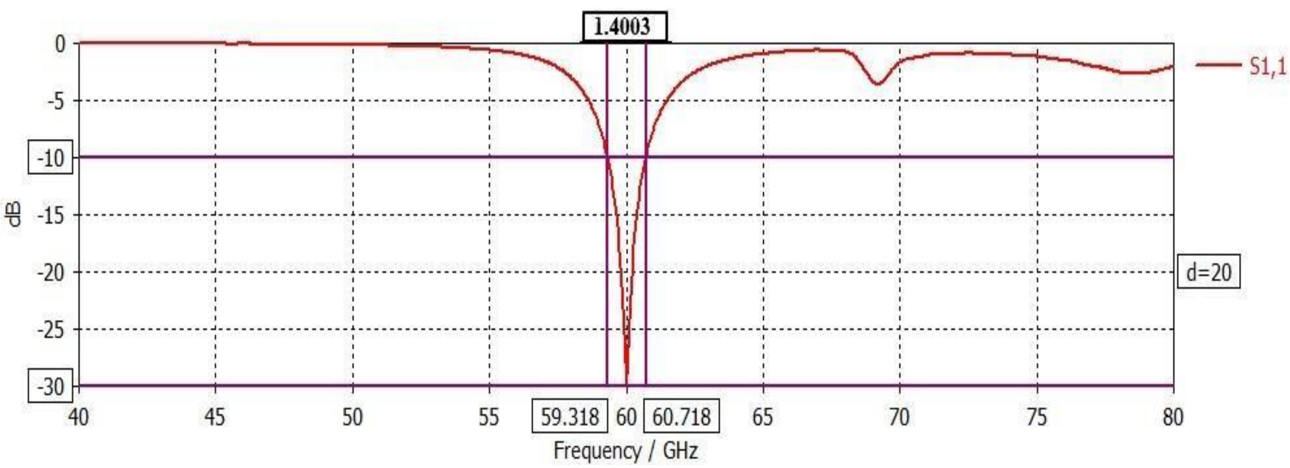

Figure 3.10: Bandwidth of the rectangular MPA with the mushroom-like EBG structure.

3.6.3 Gain

The gain for the proposed rectangular MPA with the mushroom-like EBG structure equals 7.39dBi which is better than that of the rectangular MPA, as illustrated in Figure 3.11.

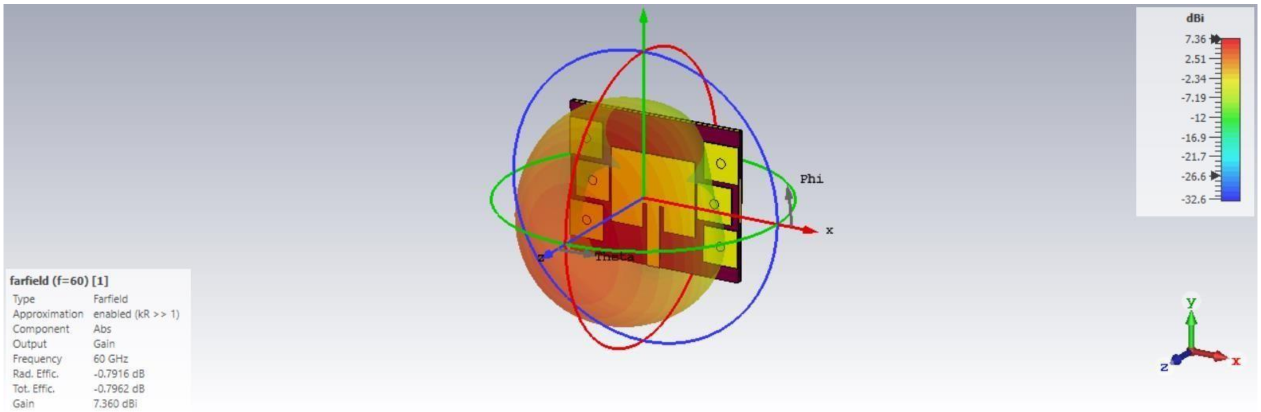

Figure 3.11: Gain for the rectangular MPA with the mushroom-like EBG structure.

3.7 FSS SUBSTRATE DESIGN

In this part, passband square loop FSS will be designed and simulated by the CST software. The fundamental intention of this procedure is to applying the "Maxwell" equations in the integral framework to a collection of reeled layers. In this work, the frequency domain solver of the CST software is utilised for modelling the spot angles of incidence. Generally, the frequency-domain solver resolves the issues for the single frequency at the time and for the number of the adaptively selected frequency units in the course of the frequency sweeping. The passband square loop FSS unit-cell within the CST environment is presented in Figure 3.12.

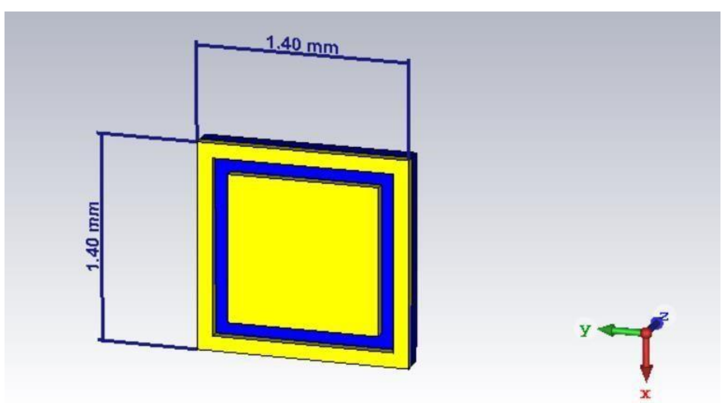

Figure 3.12: Single square loop FSS in the CST.

After testing the single-cell FSS in the CST we construct the FSS matrix by copying the single cell as an element for the matrix, as presented in Figure 3.13.

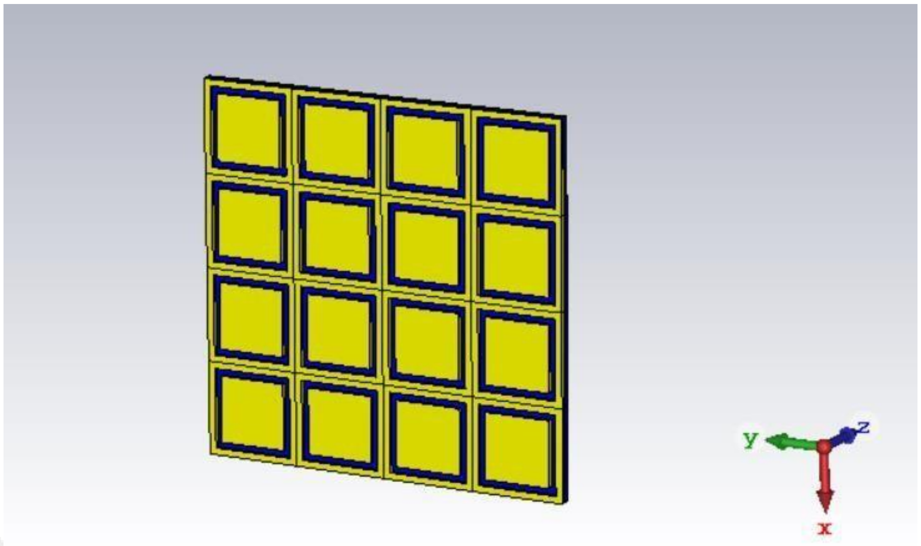

Figure 3.13: FSS matrix in the CST.

After completing the design and simulation of the FSS matrix, the designed antenna is embedded with this matrix, as illustrated in Figure 3.14.

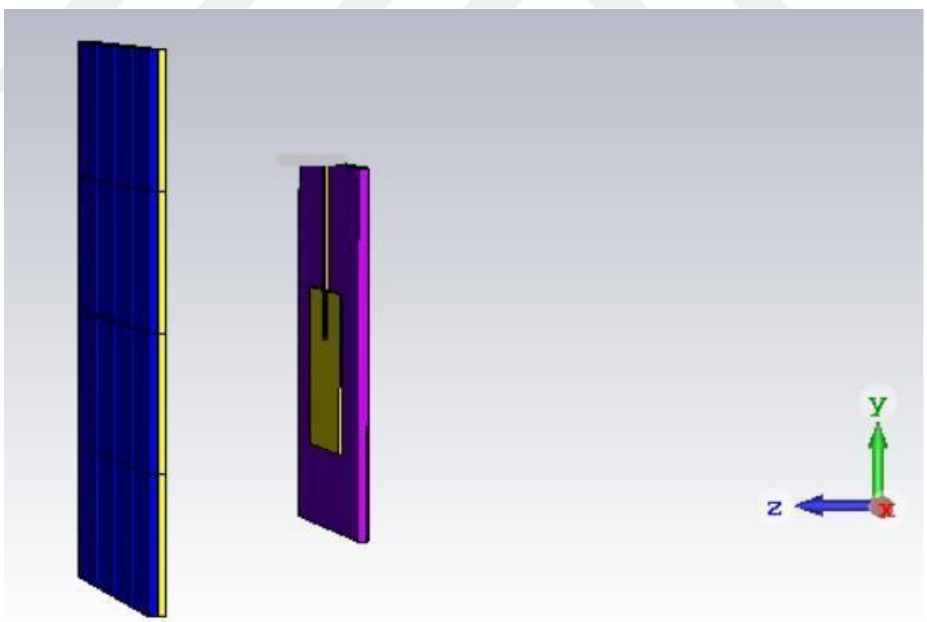

Figure 3.14: The simulated antenna with the FSS matrix.

3.8 SIMULATION RESULTS FOR THE MPA WITH FSS MATRIX

In this section of the thesis the obtained results for the designed antenna with FSS arrangement such as S_{11}, bandwidth, and antenna gain will be presented.

3.8.1 Obtained S_{11} and Bandwidth

For our utilised arrangement the FSS matrix is placed over the designed antenna with a separation gap among them. This gap is varied by trial/error till getting the best results. The selected distance for the gap for the proposed arrangement is selected to be 2.8mm. Consequently, the S_{11} is equalled to -28.23 dB, as shown in Figure 3.15. The BW is after adding the FSS matrix is improved to be about 1.6GHz, as presented in Figure 3.16.

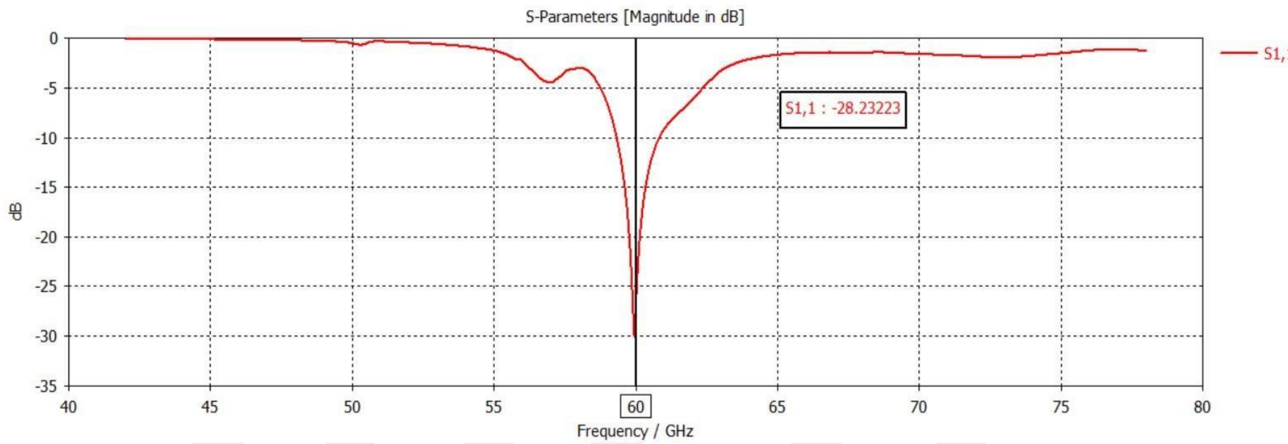

Figure 3.15: The obtained S_{11} after adding FSS matrix.

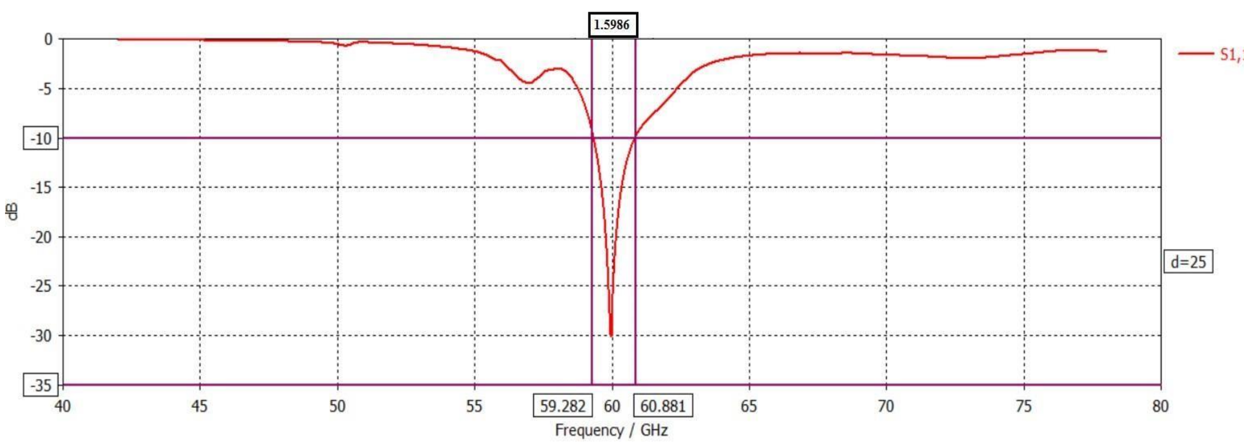

Figure 3.16: The obtained BW after adding FSS matrix.

3.8.2 Antenna Gain

After adding the FSS matrix with the designed antenna the gain is significantly enhanced to be equals to 11.8 dBi, this means that the antenna gain is improved approximately by 5 dBi than the designed antenna without the FSS matrix, as presented in Figure 3.17.

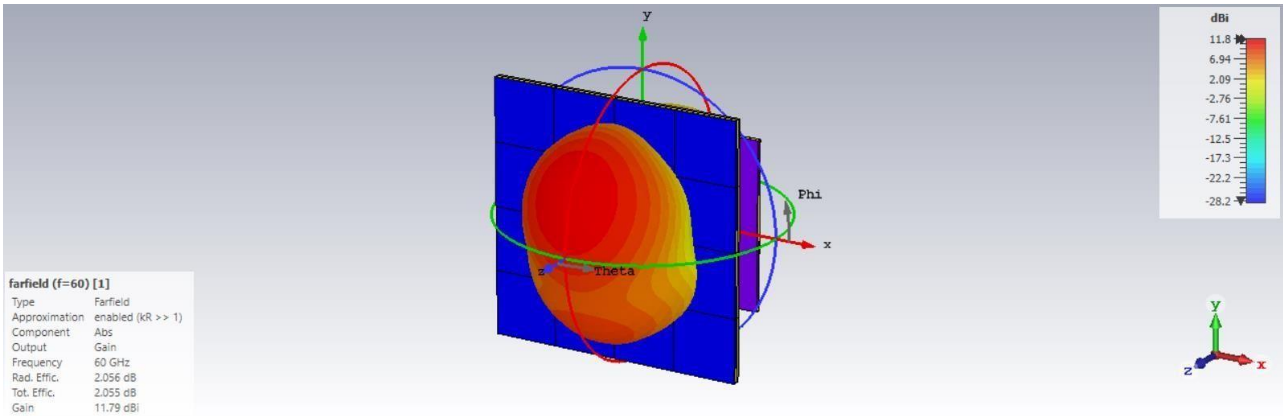

Figure 3.17: The obtained gain after adding FSS matrix.

In order to ascertain which of the methods that were used is better to improve the performance of the proposed antenna (i.e. mushroom-like EBG or FSS matrix), Table 3.4 presents a comparison of the results obtained.

Table 3.4: Comparison of the results obtained.

Parameter	**Base MPA**	**MPA with mushroom like EBG**	**MPA with FSS matrix**
S_{11} (dB)	-9.98	-29.77	-28.23
Gain (dBi)	6.87	7.39	11.8
BW (MHz)	1248	1400.3	1600
Design	Easy	Complicated	Easy

4. CONCLUSION AND FUTURE WORK

4.1 CONCLUSION

This study presented an arrangement for the mushroom-like EBG structure to avoid the bad influence of the surface wave that is produced due to the permittivity and thickness of the dielectric surface of the MPA (i.e. substrate) without wasting the miniature size that characterised the MPA.

In this work, a rectangular MPA with an inset feeding technique was loaded with cells of the mushroom like EBG structure to operate for the 60 GHz applications such as indoor applications, personal networks, or in the transfer of the HD videos/audios within an indoor range. After completed the MPA simulation a mismatching was noted at the required frequency, this issue was resolved with some shifting in the frequency by applying the optimisation process. When utilisation of the mushroom-like EBG structure, the proposed MPA operating frequency shifts to the 60GHz as required and the antenna gain was enhanced slightly. Additionally, the passive FSS structure has been proposed and designed to enhance the MPA parameter. The FSS matrix was embedded over the MPA with a distance of 2.8mm. After that, the MPA gain has been enhanced significantly to be 11.8dBi.

4.2 FUTURE WORK

There are many of additions and modifications that can be applied with the designed antenna, some of the advice can be listed as follows:

a) Fabricated the MPA with mushroom like EBG and FSS matrix and testing their performance.
b) Embedding the tunning property by the PIN diode, varactors, or the tunable materials to creating reconfigurable antenna with good performance.
c) Increase the number of the mushroom like EBG and study the MPA performance.

REFERENCES

[1] Dornan, A., & Dornan, A., "The essential guide to wireless communications applications", Prentice-Hall, 2000.

[2] Banday, Y., Rather, G. M., & Begh, G. R., "Effect of atmospheric absorption on millimetre wave frequencies for 5G cellular networks", IET Communications, vol.13, no.3, pp.265270, 2019.

[3] Daniels, R. C., & Heath, R. W., "60 GHz wireless communications: Emerging requirements and design recommendations", IEEE Vehicular technology magazine, vol.2, no.3, pp.4150, 2007.

[4] Huang, K. C., & Edwards, D. J., "Millimetre wave antennas for gigabit wireless communications: a practical guide to design and analysis in a system context", John Wiley & Sons, 2008.

[5] Chahat, N., Zhadobov, M., Le Coq, L., Alekseev, S. I., & Sauleau, R., "Characterization of the interactions between a 60-GHz antenna and the human body in an off-body scenario", IEEE Transactions on Antennas and Propagation, vol.60, no.12, pp.5958-5965, .2102

[6] Boulogeorgos, A. A. A., Alexiou, A., Merkle, T., Schubert, C., Elschner, R., Katsiotis, A., & Rodrigues, F., "Terahertz technologies to deliver optical network quality of experience in wireless systems beyond 5G", IEEE Communications Magazine, vol.56, no.6, pp.144151, 2018.

[7] Agubor, C. K., Akwukwuegbu, I., Olubiwe, M., Nosiri, C. O., Ehinomen, A., Olukunle, A. A.,& Okeke, B. C., "A comprehensive review on the feasibility and challenges of millimeter wave in emerging 5G mobile communication", Adv. Sci. Technol. Eng. Syst, vol.4, no.3, pp.138-144, 2019.

[8] Keusgen, W., Weiler, R. J., Peter, M., Wisotzki, M., & Göktepe, B., "Propagation measurements and simulations for millimeter-wave mobile access in a busy urban environment", In 2014 39th International Conference on Infrared, Millimeter, and Terahertz waves (IRMMW-THz), IEEE, pp. 1-3, 2014.

[9] Daniels, R. C., & Heath, R. W., "60 GHz wireless communications: Emerging requirements and design recommendations", IEEE Vehicular technology magazine, vol.2, no.3, pp.4150, 2007.

[10] Guo, N., Qiu, R. C., Mo, S. S., & Takahashi, K., "60-GHz millimetre-wave radio: Principle, technology, and new results", EURASIP Journal on Wireless Communications and Networking, vol. 5, no.2, pp.1-8, 2006.

[11] Ziegler, V., Schulte, B., Sabater, J., Bovelli, S., Kunisch, J., Maulwurf, K., & Grass, E., "Broadband 57–64-GHz WLAN communication system integrated into an aircraft cabin", IEEE transactions on microwave theory and techniques, vol.60, no.12, pp. 4209-4219, 2019.

[12] Alam, M. S., Islam, M. T., Misran, N., & Mandeep, J. S., "A wideband microstrip patch antenna for 60 GHz wireless applications", Elektronika ir Elektrotechnika, vol.19, no.9, pp.65-70, 2013.

[13] Rabbani, M. S., & Ghafouri Shiraz, H., "Improvement of microstrip patch antenna gain and bandwidth at 60 GHz and X bands for wireless applications", IET Microwaves, Antennas & Propagation, vol.10, no.11, pp. 1167-1173, 2016.

[14] Abdel-Wahab, W. M., & Safavi-Naeini, S., "Wide-bandwidth 60-GHz aperture-coupled microstrip patch antennas (MPAs) fed by substrate integrated waveguide (SIW)", IEEE Antennas and Wireless Propagation Letters, vol.10, pp.1003-1005, 2011.

[15] Sharaf, M. H., Zaki, A. I., Hamad, R. K., & Omar, M. M., " A novel dual-band (38/60 GHz) patch antenna for 5G mobile handsets", Sensors, vol.20, no.9, 1-19, 2020.

[16] Zarifi, D., Farahbakhsh, A., & Zaman, A. U., "A gap waveguide-fed wideband patch antenna array for 60-GHz applications", IEEE Transactions on Antennas and Propagation, vol.65, no.9, pp.4875-4879, 2017.

[17] Abdulhameed, M. K., Isa, M. M., Zakaria, Z., Mohsin, M. K., & Attiah, M. L., "Mushroomlike EBG to improve patch antenna performance for C-band satellite application", International Journal of Electrical and Computer Engineering, vol.8, no.5, pp.3875-3881, 2018.

[18] Stutzman, W. L., & Thiele, G. A., "Antenna theory and design", John Wiley & Sons, .2012

[19] Abdelaziz, A., "Bandwidth enhansment of microstrip antenna", Progress In Electromagnetics Research, vol.63, pp.311-317, 2006.

[20] Lo, Y. T., & Lee, S. W., "Antenna Handbook: theory, applications, and design", Springer Science & Business Media, 2013.

[21] Kishk, A. A., "Fundamentals of antennas. In Antennas for base stations in wireless communications", McGraw Hill Companies, 2009.

[22] Balanis, C. A. (Ed.), "Modern antenna handbook", John Wiley & Sons, 2011.

[23] Da Xu, K., Xu, H., Liu, Y., Li, J., & Liu, Q. H., "Microstrip patch antennas with multiple parasitic patches and shorting vias for bandwidth enhancement", IEEE Access, vol.6, pp.11624-11633, 2018.

[24] Shandal, S. A., Mezaal, Y. S., Mosleh, M. F., & Kadim, M. A., "Miniaturized Wideband Microstrip Antenna for Recent Wireless Applications", Advanced Electromagnetics, vol.7, no.5, pp. 7-13, 2018.

[25] Akinola, S., Hashimu, I., & Singh, G., "Gain and bandwidth enhancement techniques of microstrip antenna: a technical review", In 2019 International Conference on Computational Intelligence and Knowledge Economy (ICCIKE), IEEE, pp. 175-180, 2018.

[26] Mokal, M. V., Gagare, P. S., & Labade, D. R., "Analysis of Microstrip patch Antenna Using Coaxial feed and Micro stripline feed for Wireless Application", IOSR Journal of Electronics and Communication Engineering (IOSR-JECE), vol.12, no.3, pp.36-41, 2017.

[27] Bhattacharya, A., Dasgupta, B., & Jyoti, R., "Design and analysis of ultrathin X_band frequency selective surface structure for gain enhancement of hybrid antenna", International Journal of RF and Microwave Computer_Aided Engineering, vol.31, no.2, pp. 1-12, .2021

[28] Sofi, M. A., Saurav, K., & Koul, S. K., "Frequency-selective surface-based compact single substrate layer dual-band transmission-type linear-to-circular polarization converter", IEEE Transactions on Microwave Theory and Techniques, vol.68, no.10, pp.4138-4149, 2020.

[29] Pirhadi, A., Bahrami, H., & Nasri, J., "Wideband high directive aperture coupled microstrip antenna design by using a FSS superstrate layer", IEEE transactions on antennas and propagation, vol.60, no.4, pp.2101-2106, 2012.

[30] Abdulhameed, M. K., Isa, M. M., Ibrahim, I. M., Zin, M. S. I. M., Zakaria, Z., Mohsin, M. K., & Alrifaie, M. F., "Review of radiation pattern control characteristics for the microstrip antenna based on electromagnetic band gap (EBG)", Journal of Telecommunication, Electronic and Computer Engineering (JTEC), vol.10, no.3, pp.129-140, .2018

[31] Melouki, N., Hocini, A., & Denidni, T. A., "Performance enhancement of a compact patch antenna using an optimized EBG structure", Chinese Journal of Physics, vol.69, pp.219-229, 2021.

[32] Singh, D., Thakur, A., & Srivastava, V. M., "Miniaturization and Gain Enhancement of Microstrip Patch Antenna Using Defected Ground with EBG. J. Commun., vol.13, no.12, pp.730-736, 2018.

[33] Naderi, M., Zarrabi, F. B., Jafari, F. S., & Ebrahimi, S., "Fractal EBG structure for shielding and reducing the mutual coupling in microstrip patch antenna array", AEUInternational Journal of Electronics and Communications, vol.93, pp.261-267, 2018.

[34] Abdulhameed, M. K., Isa, M. M., Zakaria, Z., Ibrahim, I. M., Mohsen, M. K., Dinar, A. M., & Attiah, M. L., "Novel design of triple-band EBG", Telkomnika, vol.17, no.4, pp.16831691, 2019.

[35] Reddy, M. H., Joany, R. M., Reddy, M. J., Sugadev, M., & Logashanmugam, E., "Bandwidth enhancement of microstrip patch antenna using parasitic patch", In 2017 IEEE international conference on smart technologies and management for computing, communication, controls, energy and materials (ICSTM), IEEE, pp. 295-298, 2017.

[36] Khan, A., & Nema, R., "Analysis of five different dielectric substrates on microstrip patch antenna", International journal of computer applications, vol.55, no.14, pp.1123- 1128, .2012